Journal of Hydrology: Regional Studies 34 (2021) 100805

Contents lists available at ScienceDirect

Journal of Hydrology: Regional Studies

journal homepage: www.elsevier.com/locate/ejrh

Climate change impact on streamflow in a tropical basin of Ghana, West Africa

Alfred Awotwi [a,b,*], Thompson Annor [c], Geophrey K. Anornu [b], Jonathan Arthur Quaye-Ballard [d], Jacob Agyekum [c], Boateng Ampadu [a], Isaac K. Nti [e], Maxwell Anim Gyampo [f], Ebenezer Boakye [g]

[a] Department of Earth and Environmental Science, CK Tedam University of Technology and Applied Sciences (CKT-UTAS), Navrongo, Ghana
[b] Regional Water and Environmental Sanitation Centre Kumasi (RWESCK), World Bank's Africa Centre of Excellence Project, Department of Civil Engineering, Kwame Nkrumah University of Science and Technology (KNUST), Kumasi, Ghana
[c] Department of Physics, Kwame Nkrumah University of Science and Technology (KNUST), Kumasi, Ghana
[d] Department of Geomatic Engineering, Kwame Nkrumah University of Science and Technology (KNUST), Kumasi, Ghana
[e] Information Systems Department, NorthTec, Auckland, New Zealand
[f] Department of Earth Science, CK Tedam University of Technology and Applied Sciences (CKT-UTAS), Navrongo, Ghana
[g] Department of Civil Engineering, Takoradi Technical University (TTU), Takoradi, Ghana

ARTICLE INFO

Keywords:
Weighting, scaling and ranking techniques
Climate impact
Hydrological model
Streamflow
Pra River Basin

ABSTRACT

Study region: Pra River Basin, Ghana, West Africa.
Study focus: In this study, variations of the future streamflow in the Pra River Basin (PRB), are projected using the Soil and Water Analysis Tool (SWAT) model with bias-corrected climate data from regional climate models (RCMs) for the near 21 st century (2010–2039), the mid 21 st century (2040–2069), and the end of the 21 st century (2070–2099), under two Representative Concentration Pathways (RCP4.5 and RCP8.5). Weighting, scaling and ranking techniques were applied to the data from each of the seventeen climate stations to select the climate models that best reproduced the observation dataset.
New hydrological insights for the region: The results from the calibration and validation (R^2 and NSE > 0.75, and PBIAS within ± 10 %), revealed good simulation of the PRB hydrology from the SWAT model. Annually, streamflow in the near and the mid-21st century is projected to increase within 4 % and 12 % while a reduction was projected at the end of the 21 st century with the RCP4.5 emission scenario. The simulation results from the RCP8.5 scenario showed increase streamflow throughout the 21 st century applying the best performing models. Monthly streamflow variations varied between -15 % and 23 % for RCP4.5, and -24 % to 24 % for RCP8.5. Generally, increasing streamflow was highest in the RCP4.5 emission scenario. In view of the model outcomes, the PRB is expected to experience upsurge in streamflow by the near and the mid of the 21 st century. This would require proper planning by applying cost-effective adaptative water management strategies to provide for the probable influence of climate change on the future water resources of the basin.

* Corresponding author at: Department of Earth and Environmental Science, CK Tedam University of Technology and Applied Sciences (CKT-UTAS), Navrongo, Ghana.
E-mail address: awor73@yahoo.com (A. Awotwi).

https://doi.org/10.1016/j.ejrh.2021.100805
Received 4 September 2020; Received in revised form 15 February 2021; Accepted 5 March 2021
Available online 12 March 2021

1. Introduction

Increasing temperature based on RCMs data portrays that hydrological cycle might be altered as a result of increase in the water holding capacity of the atmosphere. This will result in an upsurge of the quantity of renewable fresh-water resources (He et al., 2017; Hu and Gao, 2019; Piani et al., 2010). According to Piani et al. (2010) an increase in temperature for some regions may lead to reduction in precipitation, linked to intensification in the seasonal cycle as well as frequency of extreme events. This result suggests the existence of high uncertainties in the projected effects of increasing temperatures on the hydrology for some regions (Salack et al., 2015).

The reliability of RCMs over West Africa depends on their capability to reproduce observed climate data. Accurate modeling of many climate parameters however, remains a challenging task for one particular RCM (Kabuya et al., 2020: Szabó-Takács et al., 2019; Shrestha et al., 2017; Schilling et al., 2012), since each RCM simulates the individual climate parameter differently. Hydrological components response to climate change signal therefore, appears unclear for West Africa. Moreover, most future climate impact assessment studies have been conducted with climate data from each climatic gauge stations derived from only one climate model output. Since the input components for climate models like land surface, vegetation dynamics, atmosphere, sulphate and non-sulphate aerosols, sea and oceans, vary at each climate gauge station, using one output model may not be the best to reproduce the observed climate dataset at each climate gauge station for large basins. This study therefore employed multi-criteria evaluation (MCE) to assess all the CORDEX-Africa model data at each climate gauge station. Using the multi-criteria evaluation (MCE), the best three models (best (B), second best (S) and third best (T)) for each gauge station were used to form three groups of scenarios for hydrological impact assessment in the PRB.

The PRB consists of rivers, streams, and forest areas which route large volumes of water. It controls carbon and nutrient biogeochemistry, and discharge carbon dioxide and methane into the atmosphere. The basin supports various ecosystems and socio-economic activities. Apart from the normal anthropogenic global warming activities such as urban expansions, industrialization and expansion in agriculture at the expense of forest areas, the PRB is experiencing uncontrolled rapid illegal and small-scale mining activities which are other sources of anthropogenic global warming. In recent times, the basin has encountered seasonal inadequacy in water availability making it one of the fastest water declining river basins globally (Awotwi et al., 2018; Water Resources Commission, 2012; Kusimi et al., 2014; Bessah et al., 2019). Thus, there is a need to present accurate projections about the effect of future climate change on hydrological components within the PRB for planning and managing the natural water resources for sustainable development.

Though previous researches have evaluated the effects of projected climate change on water resources in West Africa (Tall et al.,

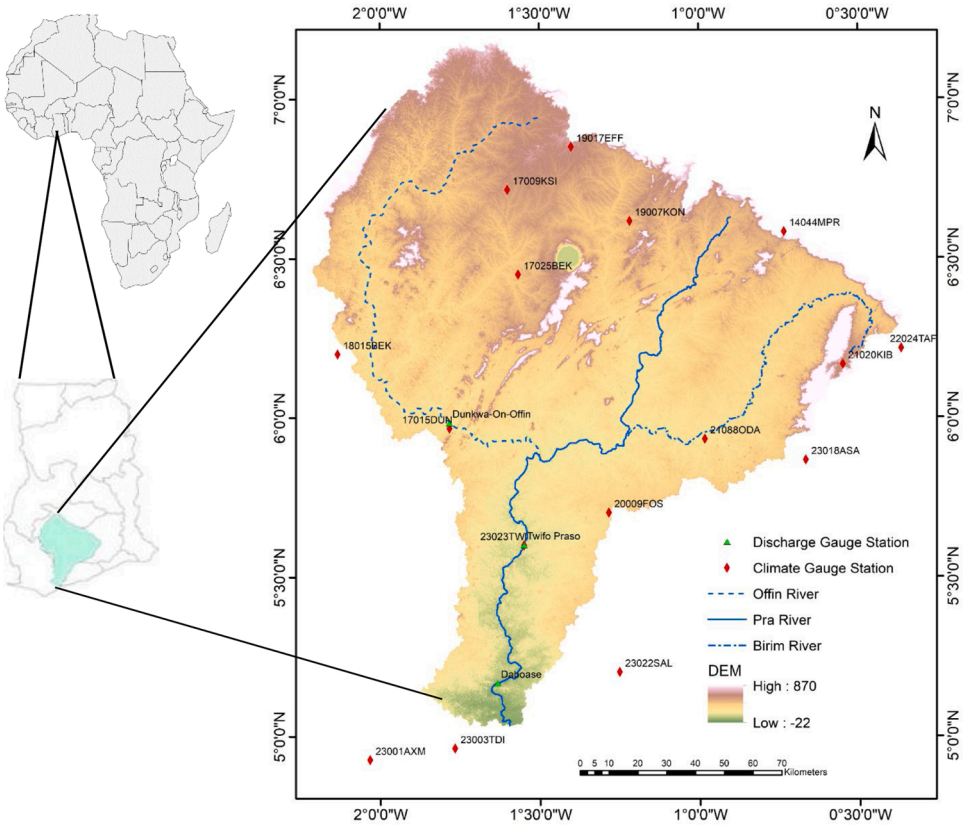

Fig. 1. Location of the study area, and meteorological and hydro-gauging stations in the Pra River Basin.

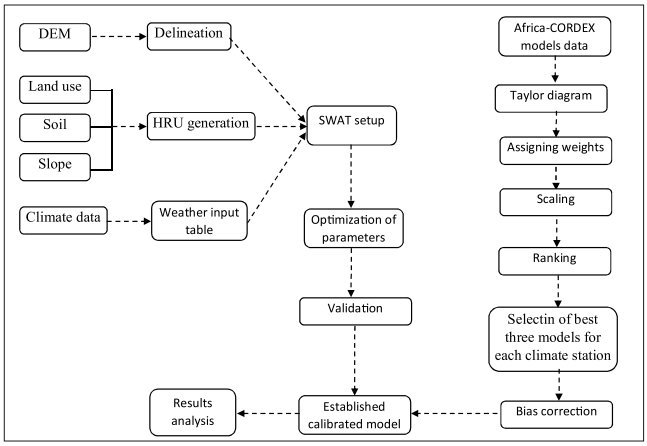

Fig. 2. Flowchart of methodology used for this study.

2017; Abubakari et al., 2018; Jin et al., 2018; Mbaye et al., 2016), all relied on simulated hydrological components based on climate data simulated by a single RCM for the entire study areas.

This study broadly aims at estimating the future climate change influence on streamflow of the PRB in Ghana, West Africa, by applying a wider dataset that will contribute to a meaningful knowledge for the planning and managing water resources in the region with sustainable developmental plans. To accomplish this aim: (1) all the CO-ordinated Regional climate Downscaling Experiment (CORDEX-Africa) RCMs were evaluated at each climate station using MCE to select the RCMs which best reproduce the observed data; (2) assess the climate change signal for the near 21 st century, mid-21st century, and the end of the 21 st century while comparing it to the base period 1971–2005; and (3) evaluate the effects of climate change on the streamflow in the PRB for the rest of the 21 st century using SWAT hydrologic model. In West Africa, the SWAT model has been effectively used in hydrological assessments (Jin et al., 2018; Awotwi et al., 2015b; Kankam-Yeboah et al., 2013; Mahé, 2009) and therefore has the capability to simulate reliable hydrological components.

The outcomes obtained from this research are likely to give more understanding into the future water availability and to offer local water management agencies and policy makers with the quantifiable data for the suitable design, management and the sustainability of water resources by factoring in climate adaptation policies to minimize vulnerability and guarantee water security for present and future generations.

Design of adaptation policies to solve the possible effects of climate change on water resource structures is a substantial challenge for stakeholders in the water resources industry (Rashid et al., 2019; Dube and Nhamo, 2019; Hirpa et al., 2018; Kumar et al., 2017; Noi and Nitivattananon, 2015; Hassanzadeh et al., 2016). According to the Fifth Assessments Report of the IPCC (2014), the West African sub-region shows little adaptive capability though it is extremely exposed to climate change. Projections for the 21 st century show austere effects of climate change on hydrology in the sub-region. These include an upsurge in the risk of water stress and flood, (Yomo et al., 2019; Serdeczny et al., 2017; Acharya and Prakash, 2019) and vital alterations in river discharge (Khandekar et al., 2019; Sassi et al., 2019; Aich et al., 2016).

2. Materials and methods

2.1. Study area

The PRB (Fig. 1) is located in the south-central part of Ghana and drains about 23,256.4 km^2. The main Pra River takes its source from the uplands of the Kwahu Plateau in the Eastern Region and flows for about 240 km before joining the Atlantic Ocean near Shama in the Western Region after travelling through four administrative regions; Eastern, Ashanti, Western and Central (Water Resources Commission, 2012), with annual discharge of 214m^3/s (Akrasi and Ansa-Asare, 2008). It consists of four major tributaries (Birim, Offin, Anum and Oda rivers) and densest network of streams. Besides the river network, it contains the only notable natural freshwater lake in Ghana (Lake Bosomtwe). The PRB is one of the most widely and severely altered river basins in Ghana due to expansion in settlement, mining, agriculture and logging as a result of its high mineral deposits and economic tree species and its favorable farming environment (Awotwi et al., 2018). The vegetative cover of the basin had and still go through a rapid rate of deforestation attributable to these anthropogenic activities. The basin experiences a sub-equatorial climate with double rainy seasons; May-July as the major season, and September-November as the minor season (Awotwi et al., 2017).

Spatially, precipitation pattern increases from the north to south of the PRB with a yearly mean precipitation of 1550 mm. The mean minimum and maximum air temperatures are 23 °C and 33 °C respectively. Air temperature decreases towards the southern part of the PRB (Awotwi et al., 2017). The southern section of the basin is relatively flat while the mid to northern sections consist of few peaks with broad river valleys. The PRB further consists of extensive agricultural lands, uncontrolled mining activities, urban and rural settlement, and industries which use large volumes of water. These factors make evaluating the effect of future climate change on the

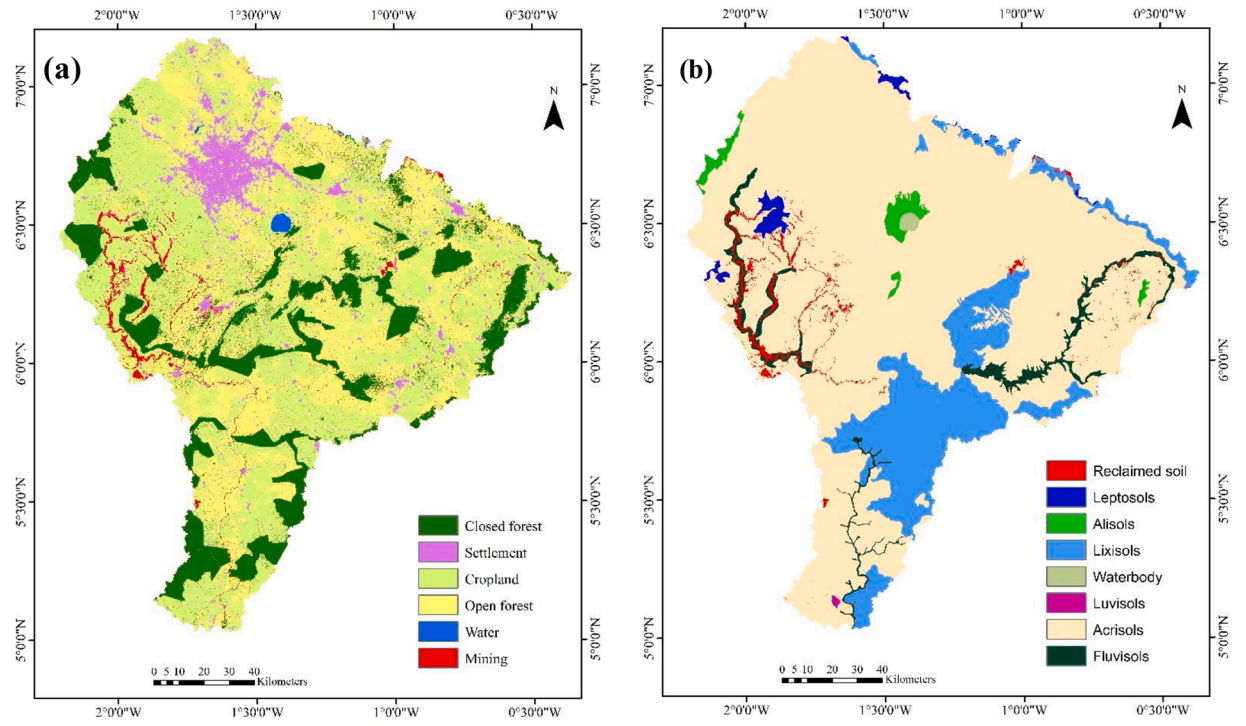

Fig. 3. SWAT model input data (a) land use map and (b) soil map.

local hydrology in the study area exceedingly important to help outline effective, efficient and sustainable water resources management programs to guarantee availability of water for present and future generations.

2.2. SWAT model input components

The SWAT model needs topographic, soil types and land use (static data) and hydro-meteorological data (dynamic data) (Fig. 2) to setup the model.

2.2.1. Digital elevation model

The SWAT model needs topographic information for delineation of watershed and depicting of drainage trends of the land surface. The DEM (1:1000,000) at 30 m resolution obtained from Shuttle Radar Topography Mission (SRTM) was corrected for sinks.

2.2.2. Land use/land cover types

The PRB land use map needed by the hydrological model for HRUs generation was obtained from the hybrid classification of 2016 Enhanced Thematic Mapper (ETM+) Landsat image. LULC information is vital for water resources analysis and especially for modeling hydrological processes (Fig. 3a).

2.2.3. Soil types

The Soil types map (Fig. 3b) and its properties were obtained from the Council for Scientific and Industrial Research, Ghana, soil database and the United Nation's Food and Agriculture (FAO) soil database. In all, six soil types were identified in the study area with acrisols covering over 75 % of the PRB. The rest of the soil types are luvisols, lixisols, fluvisols, leptosols and reclaimed soil.

2.2.4. Observed climate data

Daily time series precipitation and air temperatures (minimum and maximum) data for a period of 40 years; 1970–2010 were obtained from the Ghana Meteorological Agency (Gmet) at seventeen climatic stations situated within and close to the basin. But there were missing values in the data; on average, less than 7% for both precipitation and temperature. The correlation weighting interpolated technique was used to estimate the missing values of climate data from some meteorological stations.

2.3. Homogeneity analysis of precipitation data

As a result of changes in observational and measurement procedures, environment landscapes and edifices, and relocation of climate stations, climate datasets could show inhomogeneity. Therefore, homogenization analysis on climate data is a significant

Table 1
Overview of the IDs of Regional Climate Models considered and adopted.

Institution	RCM	Driving Model	Adopted ID
Climate Limited-Area Modelling Community (CLMcom)	CCLM4−8-17	CNRM-CM5	CCL1
Climate Limited-Area Modelling Community (CLMcom)	CCLM4−8-17	MOHC-HadGEM2-ES	CCL2
Climate Limited-Area Modelling Community (CLMcom)	CCLM4−8-17	MPI-M-MPI-ESM-LR	CCL3
Université du Québec à Montréal (UQAM)	CRCM5	CCCma-CanESM2	CRC1
Université du Québec à Montréal (UQAM)	CRCM5	MPI-M-MPI-ESM-LR	CRC2
Danish Meteorological Institute (DMI)	HIRHAM5	NCC-NorESM1-M	HI R
Royal Netherlands Meteorological Institute (KNMI)	RACMO22T	ICHEC-EC-EARTH	RAC1
Royal Netherlands Meteorological Institute (KNMI)	RACMO22T	MOHC-HadGEM2-ES	RAC2
Swedish Meteorological and Hydrological Institute (SMHI)	RCA4	CCCma-CanESM2	RCA1
Swedish Meteorological and Hydrological Institute (SMHI)	RCA4	CNRM-CERFACS-CNRM-CM5	RCA2
Swedish Meteorological and Hydrological Institute (SMHI)	RCA4	CSIRO-QCCCE-CSIRO-Mk3−6-0	RCA3
Swedish Meteorological and Hydrological Institute (SMHI)	RCA4	MOHC-HadGEM2-ES	RCA4
Swedish Meteorological and Hydrological Institute (SMHI)	RCA4	MIROC-MIROC5	RCA5
Swedish Meteorological and Hydrological Institute (SMHI)	RCA4	MPI-M-MPI-ESM-LR	RCA6
Swedish Meteorological and Hydrological Institute (SMHI)	RCA4	NCC-NorESM1-M	RCA7
Swedish Meteorological and Hydrological Institute (SMHI)	RCA4	NOAA-GFDL-GFDL-ESM2M	RCA8
Climate Service Centre in Hamburg, Germany (CSC)	REMO	IPSL-IPSL-CM5A	REM1
Climate Service Centre in Hamburg, Germany (CSC)	REMO	MIROC-MIROC5	REM2
Climate Service Centre in Hamburg, Germany (CSC)	REMO	MOHC-HadGEM2-ES	REM3
Climate Service Centre in Hamburg, Germany (CSC)	REMO	MPI-M-MPI-ESM-LR	REM4
Climate Service Centre in Hamburg, Germany (CSC)	REMO	NOAA-GFDL-GFDL-ESM2G	REM5

procedure to identify the changeability in the data. This study used the standard normal homogeneity test (SNHT) proposed by Alexandersson (1986) to assess the homogeneity.

Per the null hypothesis, the yearly values Pi of the testing variables P are independent and evenly distributed therefore, the data is termed homogeneous. Alternative hypothesis test presume that the data involves discontinuity in the mean and termed inhomogeneous.

The statistic S(p) which matches the average of the first p years to (n-p) years is evaluated by:

$$S_p = p\bar{z}_1 + (n-p)\bar{z}_2, \; p = 1, 2, 3, 4, \ldots\ldots\ldots\ldots n \tag{1}$$

Where

$$\bar{z}_1 = \frac{1}{p}\sum_{i=1}^{n}\frac{\left(P_i - \overline{P}\right)}{\sigma} \; and \; \bar{z}_2 = \frac{1}{n-p}\sum_{i=p+1}^{n}\frac{\left(P_i - \overline{P}\right)}{\sigma} \tag{2}$$

$\overline{P}$ and σ = average and the standard deviation respectively.

The year p is said to consist of break if the value of S is maximum. To reject null hypothesis, the test statistic,

$$S_0 = \max_{1\le p\le n} S_p \tag{3}$$

is greater than the critical value, which is based on the sample size.

The method proposed by Wijngaard et al. (2003) was used to evaluate the homogeneity of the precipitation data at each climate station and using yearly average and yearly maximum as testing variables. The yearly mean and maximum precipitation of each climate station were examined for homogeneity utilizing a critical value of 6.95 proposed by Wijngaard et al. (2003).

2.4. Model calibration and validation of flow discharge

Some parameters used by hydrological models cannot be measured directly in the field. These parameters need to be adjusted to enhance the concurrence between observed and simulated values. For this work the calibration and validation were done using a 31 year period daily observed discharge data (1 st January 1980 – 31st December 2010) at the Daboase gauge station, the outlet of the PRB, obtained from Ghana Hydrological Service. However, there were missing values in the observed data which were less than 4% of the observed data. Three years' data (1st January 1980 – 31st December 1982) were used to warm-up the model, while that of 1st January 1983 – 31st December 1998 and 1st January 1999 – 31st December 2010 were used for calibration and validation respectively. Employing a manual calibration method, the model parameters were adjusted until the modeled discharge was within the statistically suitable model performance scope. The gaps in the data were filled using the inverse distance weighting method with respect to the Dunkwa-On-Offin and Twifo Praso gauging stations. In this study, manual calibration which involves a trial and error method was adopted. It was carried out on parameters that were most sensitive during sensitivity analysis (Abubakari et al., 2018). The sensitivity analysis of the study was done with reference to the

calibration periods. On the optimization process that replicates the sensitivity of the 21 SWAT input parameters, 1500 numbers of iterations were performed in gaining the most sensitive parameters. After model calibration, 12 years discharge data from the Daboase

station (1st January 1999–31st December 2010) was used for model validation.

The reliability of the simulation was assessed statistically by four indices, Nash-Sutcliff efficiency (NSE), RMSE-observations standard deviation ratio (RSR), percent bias (PBIAS), and coefficient of determination (R^2) proposed by Nash and Sutcliffe (1970), Chu and Shirmohammadi (2004), Gupta et al. (1999), and Santhi et al. (2011) respectively. The assessment of the performance of the hydrological model is based on the statistical indicators NSE, PBIAS and RSR proposed by Moriasi et al. (2007).

2.5. Future climate change (CC) scenarios

The IPCC Representative Concentration Pathway (RCP) 4.5 and RCP 8.5 scenarios were utilized as the principal tools for future climate change assessment because RCP8.5 is considered the strongest climate signal with the greatest atmospheric greenhouse gas concentrations in the late 21 st century while RCP4.5 presumes that emissions of greenhouse gases will soon become constant and then drop after a few decades (van Vuuren et al., 2011).

Future precipitation and temperature data were obtained from outputs of nine GCMs forcing six RCMs (Table 1) from the CORDEX-Africa initiative. The objective of CORDEX-Africa is to provide high-resolution climate data for Africa. Historical simulated data, 1971–2005, was utilized as the reference epoch for this study. The impending climate is characterized for three timeline scenarios, 2010–2039 representing near 21st century (NE), 2040–2069 signifying mid 21st century (MD), and 2070–2099 indicating the end of the 21st century (ED).

2.6. Bias correction

Despite the fact that the models have been enhanced over time they still contain bias and is a source of worry in climate research. Uncorrected output from climate models makes it unreliable for effective hydrological studies therefore, the usage of bias correction methods on the downloaded simulated climate data to improve the exactness of the modeled hydrological components. To overcome this, distribution mapping (DM) bias-correcting method of CMhyd model (Rathjens et al., 2016), was used to correct the bias. This component has been extensively use in bias correction for climate change assessment studies (Schmidli et al., 2006; Olsson et al., 2015; Mbaye et al., 2016; Tschoke et al., 2017). The rationale behind this method is to fit the parameters of transfer functions of climate modeled data to that of the measured data. Gamma and Gaussian distributions (transfer functions) are used on precipitation and temperature, respectively. With the precipitation, random precipitation intensity will first of all be definite and then employed to establish the cumulative probability of modeled precipitation. After that, centered on the cumulative probability, the corrected precipitation value is chosen. While for temperature, the cumulative probability of modeled temperature data may well be established. Subsequently, based on the probability, the corrected temperature value can be chosen. According to Teutschbein and Seibert (2012), this method of bias correction yields a very good result.

2.7. Weighting and ranking of climate models

Around the globe, there are over thirty research groups that have established their own climate models. Though the foundation framework of these models is similar, they all vary in their details. In any instance, the models must depict the physical collaborations between the atmosphere, the oceans, land surfaces, and sea ice with reference to a multitude of processes functioning on various space and time scales. Climate model developers have different opinions about which physical components to emphasize. Thus, at the same time, different climate models produce different results at a location.

To produce reliable climate impact results, this study compared all the CORDEX-Africa models output data with the observed data

Table 2
Annual outcomes from SNHT-analysis of rainfall gauge stations.

No.	**Station Name**	Station ID	**Mean**	**Maximum**
1	Takoradi Airport	23003TDI	2.47	1.26
2	Axim	23001AXM	2.98	3.37
3	Dunkwa On Offin	17015DUN	2.43	2.63
4	Saltpond	23022SAL	2.14	1.59
5	Twifo Praso	23023TWI	2.70	4.90
6	Atieku	18026ATI	3.67	7.13 (2009)
7	Kibi	21020KIB	2.13	4.31
8	Tafo Akim(Crig)	22024TAF	1.92	6.18
9	Eefiduase	19017EFF	2.54	2.61
10	Bekwai Ashanti	17025BEK	5.56	5.51
11	Asamankese	23018ASA	4.37	2.94
12	Akim Oda	21088ODA	4.05	2.55
13	Kumasi Airport	17009KSI	5.88	4.94
14	Konongo	19007KON	3.40	5.30
15	Sefwi- Bekwai	18015BEK	2.74	2.08
16	Mpasaso	16016MPE	3.26	2.74
17	Assin Foso	20009FOS	3.25	2.59

Table 3
Sensitivity analysis on the 14 input parameter.

No.	SWAT input Parameter	Parameter description	t-stats	p-value	Rank
1	CN2.mgt	SCS runoff curve number	−18.41	0.000	1
2	Alpha_BF.gw	Baseflow alpha factor (days	9.76	0.000	2
3	SOL_AWC.sol	Available water capacity of the soil layer	8.63	0.000	3
4	ESCO.bsn	Soil evaporation compensation factor	6.27	0.001	4
5	GW_DELAY.gw	Groundwater delay (days)	6.01	0.001	5
6	GW_QMN.gw	Threshold depth of water in the shallow aquifer required for return flow to occur (mm)	5.81	0.002	6
7	GW_REVAP.gw	Groundwater “revap” coefficient to occur (mm)	5.45	0.002	7
8	RCHARG_DP.gw	Deep aquifer percolation fraction	3.92	0.003	8
9	CH-K2.rte	Effective hydraulic conductivity in main channel alluvium	−3.06	0.003	9
10	EPCO.bsn	Plant uptake compensation factor	3.01	0.003	10
11	REVAPMN.gw	Threshold depth of water in the shallow aquifer for “revap” to occur (mm)	2.37	0.008	11
12	CH_N2.rte	Manning’s “n” value for the main channel	−2.11	0.013	12
13	CANMX.hru	Maximum canopy storage	1.94	0.018	13
14	SURLAG.bsn	Surface runoff lag time	−1.56	0.025	14

Table 4
Parameters adjusted for calibration of the SWAT model.

SWAT input Parameter	Boundary	Final Value
CN2.mgt	35 - 98	35.2 – 58.88
Alpha_BF.gw	0 - 1	0.017
SOL_AWC.sol	0 - 1	0.12 – 0.14
ESCO.bsn	0 - 1	0.75
GW_DELAY.gw	0 - 50	28
GW_QMN.gw	0 - 5000	4900
GW_REVAP.gw	0.02 – 0.2	0.025
RCHARG_DP.gw	0 - 1	0.1
CH-K2.rte	0 - 150	54.2
EPCO.bsn	0 - 1	0.94
REVAPMN.gw	0 - 500	110
CH_N2.rte	0 - 1	0.018
CANMX.hru	0 - 10	0.4
SURLAG.bsn	0 - 10	3.8

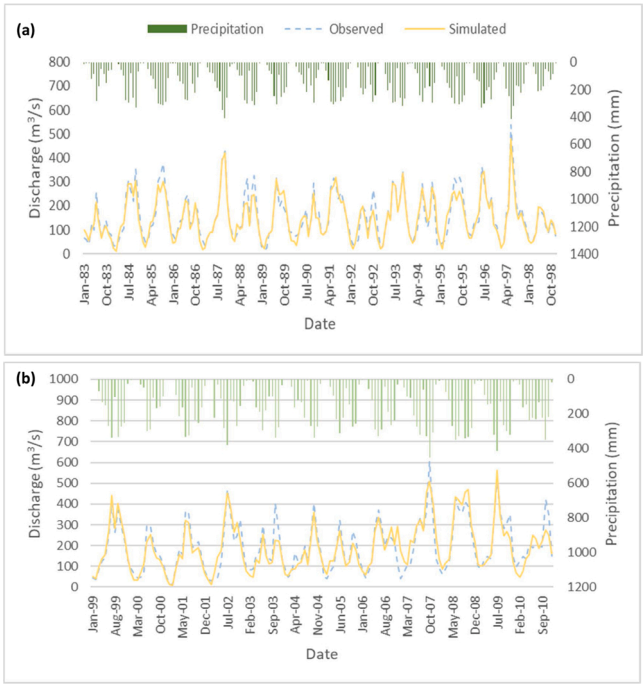

Fig. 4. Monthly streamflow for (a) calibration and (b) validation periods of the SWAT model.

Table 5
Calibration and validation performance of the SWAT model.

Stage	Statistics indicators			
	NSE	RSR	PBIAS	R^2
Calibration	0.79	0.47	−4.3	0.79
Validation	0.76	0.52	−1.0	0.76

at each climate station. This was achieved by first generating a Taylor diagram for all the CORDEX-Africa models data for each climate station (wet and dry season Taylor diagrams for minimum and maximum temperature and precipitation). The Taylor diagram offers a statistical summary of how well the modeled patterns reproduce the observed patterns in terms of mean square error (RMSE), correlation coefficient (CC) and normalized standardized deviation (NSD). It provides a diagram as a series of points on a polar plot. Consequently, all these three statistical factors should be considered at the same time with equal weight in selecting the best model.

Equal weights of 1–10 corresponding to worst to best reproduction of the observed climate dataset, were placed on RMSE, CC and NSD of each climate model at each climatic gauge station using Eqs. (6) and (7). For precipitation, the data was scaled down with 0.7 for wet season and 0.3 for dry season while temperature (maximum and minimum) were scaled by 0.5 for both wet and dry season (Fig. 2) after which the sum of the weights were taken. To institute the ranking of the climate models, it is appropriate to arrange them based on the reducing value of their closeness coefficient of summation weights. Though it was tedious, time consuming and expensive procedure, it produces highly accurate data for the impact assessment. Then, bias-correction was applied to the best three models for each station before they were used to force the hydrological model (SWAT).

Table 6
Statistical assessment of simulated mean monthly RCM precipitation under DM method.

Climate model	Data Type	Mean (mm)	Std Dev. (mm)	90th Percentile (mm)	Coefficient of Variation	Precipitation Intensity	Wet day probability	Bias	RMSE (mm)	R
OBS		127.58	9.28	13.33	2.87	11.74	0.38	–	–	–
CCL1	Raw	121.05	8.01	7.58	3.24	4.28	0.61	−0.24	84.37	0.62
	BC	127.33	10.29	12.67	2.88	12.93	0.32	−0.01	0.83	0.99
CCL2	Raw	98.91	7.12	7.67	3.37	4.55	0.69	−0.22	96.87	0.71
	BC	127.67	15.13	16.61	4.07	12.90	0.33	0.00	0.44	1.00
CCL3	Raw	126.50	7.49	7.86	3.57	4.71	0.68	−0.08	69.63	0.73
	BC	127.41	14.68	8.88	3.88	11.29	0.35	0.01	0.64	0.99
CRC1	Raw	162.16	7.59	13.18	0.768	6.31	0.79	0.27	80.30	0.46
	BC	128.00	13.52	20.11	3.41	13.11	0.33	0.00	0.57	1.00
CRC2	Raw	164.33	10.26	17.88	1.66	8.30	0.79	0.67	119.21	0.60
	BC	127.54	12.15	11.03	3.16	13.03	0.33	0.00	0.99	1.00
RAC1	Raw	131.42	3.94	8.25	1.03	4.25	0.95	0.03	141.92	0.63
	BC	127.92	11.28	19.41	3.14	13.01	0.33	0.00	0.92	0.99
RAC2	Raw	146.33	4.23	15.48	1.03	4.31	0.96	0.05	98.27	0.59
	BC	127.00	11.34	10.23	2.95	12.93	0.33	0.00	0.68	0.98
RCA1	Raw	114.25	4.48	9.37	2.72	5.26	0.62	−0.1	43.01	0.83
	BC	127.58	10.33	14.38	2.89	12.68	0.33	−0.01	0.72	1.00
RCA2	Raw	123.08	4.60	9.75	2.47	5.88	0.61	−0.04	44.89	0.83
	BC	127.54	10.11	13.01	2.68	12.07	0.37	0.02	0.05	1.00
RCA3	Raw	122.68	3.21	4.941	2.67	3.09	0.50	−0.56	100.39	0.46
	BC	127.44	11.62	11.71	3.17	13.44	0.32	−0.01	0.29	1.00
RCA4	Raw	122.33	5.45	12.03	1.46	6.35	0.62	−0.35	92.24	0.58
	BC	127.50	10.20	11.05	3.09	12.93	0.32	0.01	0.79	1.00
RCA5	Raw	127.02	5.96	12.26	1.297	6.81	0.78	0.34	62.91	0.81
	BC	128.07	10.43	19.27	3.21	11.30	0.32	0.01	0.65	0.98
RCA6	Raw	156.33	5.23	11.47	1.79	6.69	0.67	0.23	66.92	0.78
	BC	125.25	12.15	12.58	3.30	10.60	0.39	0.03	0.41	0.96
RCA7	Raw	189.58	7.78	17.28	1.38	8.61	0.70	0.31	69.82	0.43
	BC	127.58	10.64	14.01	3.04	12.85	0.33	0.00	0.74	1.00
RCA8	Raw	171.50	6.71	10.89	2.53	6.89	0.64	0.34	101.83	0.74
	BC	128.40	13.81	17.24	3.26	12.78	0.32	0.01	0.82	1.00
REM1	Raw	167.5	9.73	13.87	5.00	5.07	0.70	0.16	107.61	0.56
	BC	127.75	11.90	12.33	3.61	12.53	0.32	0.00	0.72	0.98
REM2	Raw	184.75	12.25	15.88	2.96	6.44	0.81	0.45	93.32	0.84
	BC	127.33	11.28	11.50	3.08	11.58	0.32	0.00	0.50	0.98
REM3	Raw	151.08	12.85	13.35	2.64	6.067	0.79	0.27	89.06	0.61
	BC	128.08	11.63	16.53	3.22	12.73	0.32	0.00	0.75	0.99
REM4	Raw	153.50	9.58	13.42	3.63	5.32	0.76	0.20	80.23	0.71
	BC	127.58	12.13	13.42	3.72	12.75	0.32	0.00	0.36	1.00
REM5	Raw	151.42	12.00	12.70	4.29	5.39	0.67	0.19	113.38	0.59
	BC	127.33	11.88	12.46	3.68	12.81	0.31	−0.02	0.98	0.99

Where Std. Dev = Standard deviation, R = correlation coefficient. RMSE = Root mean square error, BC = Bias corrected.

Table 7
Mean scale and shape parameters of DM.

	Observed		Simulated	
RCM	Scale	Shape	Scale	Shape
CCL1	15.06	0.78	4.31	5.19
CCL2	15.36	0.76	5.46	1.72
CCL3	15.38	0.76	4.42	2.79
CRC1	14.73	0.80	5.28	3.67
CRC2	14.70	0.81	6.11	4.03
RAC1	15.55	0.74	0.96	11.14
RAC2	15.38	0.77	1.82	6.45
RCA1	15.37	0.75	2.43	5.41
RCA2	15.38	0.76	2.58	5.14
RCA3	15.41	0.80	2.21	4.09
RCA4	14.88	0.79	1.95	8.26
RCA5	16.02	0.74	4.17	7.79
RCA6	16.21	0.71	2.83	5.66
RCA7	14.70	0.81	2.41	6.70
RCA8	14.70	0.81	3.41	4.67
REM1	14.73	0.81	8.13	1.19
REM2	14.42	0.84	8.45	1.58
REM3	15.03	0.77	15.78	1.42
REM4	14.46	0.79	8.34	1.27
REM5	15.40	10.14	0.74	1.77

Table 8
Statistical assessment of simulated mean monthly RCM maximum temperature under DM method.

Climate model		Mean (°C)	Std. Dev. (°C)	90th Percentile (°C)	Bias	RMSE (°C)	R
OBS		31.15	1.29	32.85	–	–	–
CCL1	Raw	31.06	2.40	34.74	0.02	2.55	0.90
	BC	31.14	1.30	32.70	−0.01	0.09	1.00
CCL2	Raw	30.08	3.79	35.28	−0.03	4.01	0.86
	BC	31.15	1.43	33.80	0.00	0.06	1.00
CCL3	Raw	30.04	2.02	32.63	−0.04	3.03	0.92
	BC	31.15	1.30	32.83	0.00	0.07	1.00
CRC1	Raw	32.17	1.75	34.14	0.03	1.74	0.85
	BC	31.19	1.27	33.06	0.00	0.07	1.00
CRC2	Raw	31.95	2.08	34.18	0.01	1.45	0.86
	BC	31.19	1.30	33.01	0.00	0.09	1.00
RAC1	Raw	28.48	1.37	30.16	−0.09	3.00	0.73
	BC	31.20	1.30	33.17	0.00	0.15	0.99
RAC2	Raw	29.17	2.05	31.99	0.06	3.19	0.89
	BC	31.15	1.28	32.90	0.00	0.10	1.00
RCA1	Raw	33.78	1.30	35.38	0.08	3.16	0.88
	BC	31.18	1.29	33.28	0.00	0.16	0.99
RCA2	Raw	33.24	1.48	34.98	0.07	2.63	0.89
	BC	31.22	1.29	33.17	0.00	0.13	1.00
RCA3	Raw	31.91	1.70	33.97	0.02	2.13	0.48
	BC	31.20	1.30	33.50	0.00	0.14	1.00
RCA4	Raw	32.24	2.57	35.03	0.06	3.65	0.68
	BC	31.16	1.28	32.89	0.00	0.05	1.00
RCA5	Raw	32.13	1.56	33.97	0.03	1.92	0.83
	BC	31.15	1.30	33.11	0.00	0.09	1.00
RCA6	Raw	31.70	1.44	34.42	0.02	2.38	0.77
	BC	31.20	1.28	32.75	0.00	0.08	1.00
RCA7	Raw	33.40	1.45	33.91	0.07	2.83	0.83
	BC	31.21	1.30	33.15	0.00	0.10	1.00
RCA8	Raw	32.38	1.68	33.61	0.04	2.41	0.92
	BC	31.15	1.29	32.88	0.00	0.11	1.00
REM1	Raw	33.20	2.77	36.63	0.07	3.99	0.96
	BC	31.14	1.28	32.72	0.00	0.07	1.00
REM2	Raw	33.21	2.44	35.47	0.07	3.76	0.85
	BC	31.16	1.33	32.91	0.00	0.08	1.00
REM3	Raw	32.03	4.15	37.35	0.03	3.79	0.93
	BC	31.15	1.34	32.90	0.00	0.05	1.00
REM4	Raw	32.57	2.64	35.75	0.05	2.69	0.94
	BC	31.16	1.32	33.02	0.00	006	1.00
REM5	Raw	32.11	2.825	35.43	0.03	3.98	0.96
	BC	31.16	1.30	32.92	0.00	0.10	1.00

Where Std. Dev = Standard deviation, R = correlation coefficient. RMSE = Root mean square error, BC = Bias corrected.

$$WT_{RMSE/NSD} = 10 - \lfloor (10*(RMSE_{TD}/NSD_{TD}) \div (RMSE_{TO}/NSD_{TO})) \rfloor \quad (6)$$

$$WT_{CC} = 10*CC_{TD} \quad (7)$$

Where $WT_{RMSE/NSD}$ is the weighted RMSE and NSD,
$RMSE_{TD}$, NSD_{TD} and CC_{TD} are the RMSE, NSD and CC values from the Taylor diagram respectively,
$RMSE_{TO}$ and NSD_{TO} are the total length of RMSE and NSD respectively with reference to OBS on the Taylor diagram and
WT_{CC} is the weighted CC

2.8. Uncertainty assessment

It would be ideal to have data free from uncertainties, but this is not possible. To some extent, each single data has some form of uncertainties. Therefore, there are uncertainties related to this study. According to Walker et al., 2003, uncertainty is any departure from complete deterministic knowledge of the relevant system, therefore, the uncertainty associated with this study was evaluated based on:

$$\frac{Differencees\ between\ observed\ and\ best/\ second\ best/\ third\ best,\ model}{observed} \times 100 \quad (8)$$

Table 9
Statistical assessment of simulated mean monthly RCM minimum temperature under DM method.

Climate model	Data type	Mean (°C)	Std. Dev. (°C)	90th Percentile (°C)	Bias	RMSE (°C)	R
OBS		21.51	1.62	23.41	–	–	
CCL1	Raw	21.44	1.35	23.10	−0.04	1.53	0.90
	BC	21.51	1.61	23.50	0.00	0.06	1.00
CCL2	Raw	20.08	1.39	23.01	−0.07	1.75	0.86
	BC	21.51	1.60	23.50	0.00	0.08	1.00
CCL3	Raw	21.03	1.15	23.16	−0.05	1.61	0.92
	BC	21.51	1.61	23.47	0.00	0.02	1.00
CRC1	Raw	22.46	1.33	23.96	0.05	1.32	0.85
	BC	21.52	1.63	23.58	0.00	0.08	1.00
CRC2	Raw	22.05	1.41	23.69	0.02	1.26	0.86
	BC	21.50	1.62	23.29	0.00	0.06	1.00
RAC1	Raw	20.45	1.16	21.73	−0.05	1.26	0.73
	BC	21.51	1.64	23.43	0.00	0.03	0.99
RAC2	Raw	21.09	1.44	23.22	−0.01	0.89	0.89
	BC	21.53	1.62	23.59	0.00	0.05	1.00
RCA1	Raw	23.29	1.30	24.58	0.08	2.21	0.88
	BC	21.51	1.63	23.45	0.00	0.05	0.99
RCA2	Raw	21.89	1.56	23.53	0.03	1.98	0.89
	BC	21.51	1.64	23.52	0.00	0.04	1.00
RCA3	Raw	23.19	0.85	24.29	0.08	1.76	0.48
	BC	21.51	1.63	23.52	0.00	0.08	1.00
RCA4	Raw	24.27	1.74	23.61	0.07	1.95	0.68
	BC	21.52	1.62	23.61	0.00	0.05	1.00
RCA5	Raw	22.67	1.24	23.96	0.05	1.28	0.83
	BC	21.52	1.66	23.53	0.00	0.02	1.00
RCA6	Raw	22.00	1.46	23.73	0.02	1.21	0.77
	BC	21.50	1.65	23.48	0.00	0.06	1.00
RCA7	Raw	22.73	1.33	24.28	0.06	1.54	0.83
	BC	21.51	1.63	23.41	0.00	0.05	1.00
RCA8	Raw	22.11	1.70	23.61	0.02	1.97	0.92
	BC	21.51	1.62	23.53	0.00	0.05	1.00
REM1	Raw	22.75	1.58	24.73	0.06	2.61	0.96
	BC	21.53	1.65	23.57	0.00	0.08	1.00
REM2	Raw	23.30	1.24	24.73	0.08	2.13	0.85
	BC	21.54	1.65	23.46	0.00	0.09	1.00
REM3	Raw	22.76	2.12	25.06	0.06	1.75	0.93
	BC	21.52	1.61	23.39	0.00	0.03	1.00
REM4	Raw	23.23	1.45	24.06	0.08	3.98	0.94
	BC	21.53	1.67	23.52	0.00	0.07	1.00
REM5	Raw	21.58	1.55	23.71	0.00	2.60	0.96
	BC	23.51	1.65	23.31	0.00	0.09	1.00

Where Std. Dev = Standard deviation, R = correlation coefficient. RMSE = Root mean square error, BC = Bias corrected.

3. Results and discussion

3.1. Precipitation homogeneity

From Table 2, the entire seventeen stations reveled homogeneity in their precipitation under the testing variable of annual mean, as the null hypothesis under the SNHT is not rejected at 0.05 level of significance. Whiles only one climate station precipitation data out of the seventeen stations portrayed homogeneity under the yearly maximum testing variable. Although inhomogeneous station was detected, the outcomes are suitable since there is no much variation. Hence, the stations can be used for further assessment.

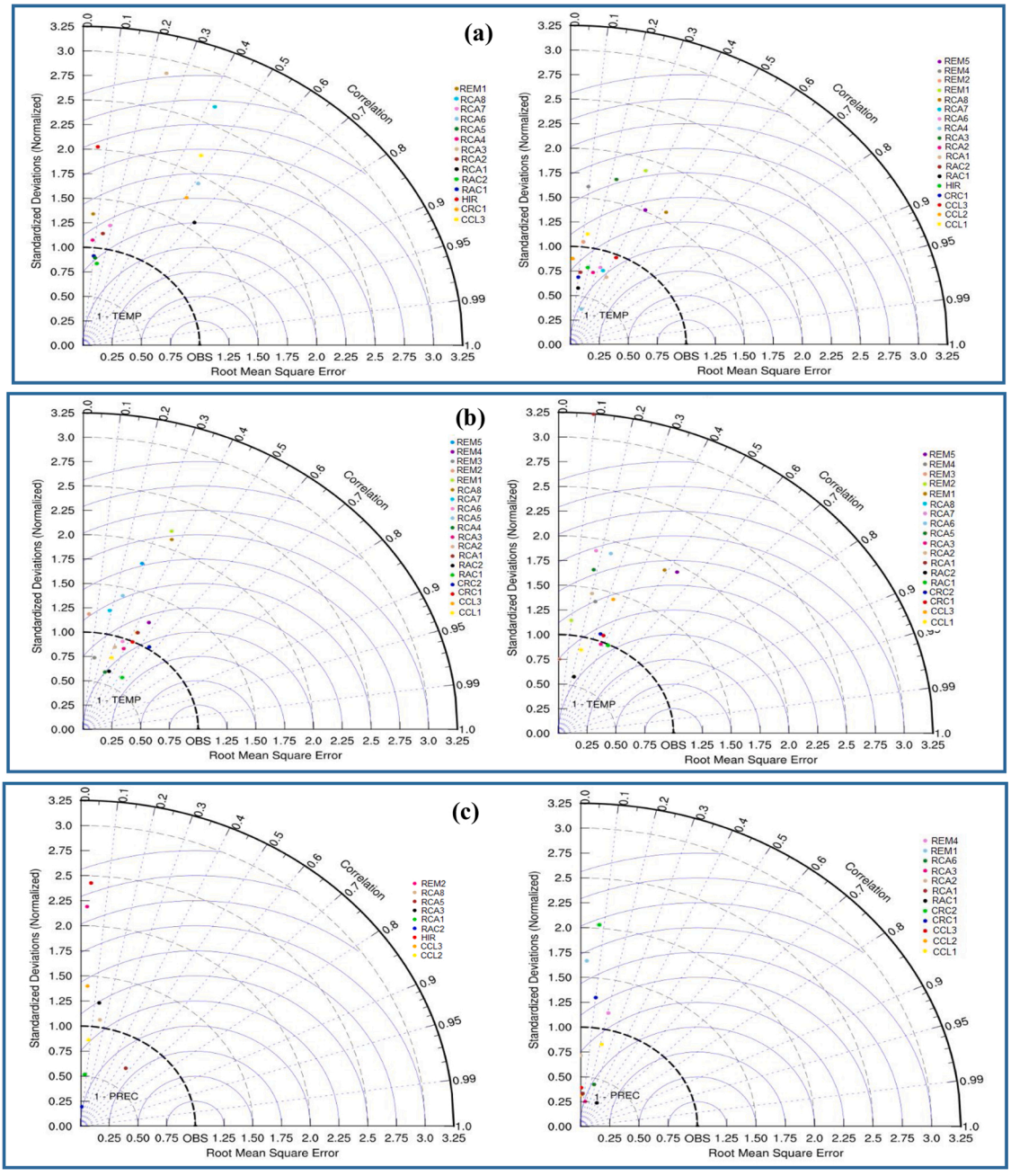

Fig. 5. Taylor diagram for the Kumasi (left) and Takoradi (right) climate stations depicting the normalized standard deviation, the correlation, and the RMSE within the (a) Maximum temperature (b) Minimum temperature (c) Rainfall, models and the baseline data.

3.2. Calibration and validation of SWAT

The fourteen most sensitive parameters out of 21 obtained from the sensitivity analysis are shown in Table 3. The SCS runoff curve number (CN2) was found to be the most sensitive parameters for the PRB. The final adjusted final values during calibration are shown in Table 4. These parameters are substantially linked to surface runoff. The comparisons of measured and simulated hydrographs for the calibration and validation epochs are shown in Fig. 4. The overestimation and underestimation of the simulated discharge might be due to the mistakes in measuring the input data as well as errors associated with the SWAT model. The underestimation of the low flows may be as a result of more than one aquifer contributing to baseflow which is not dealt with in the SWAT model.

The graphs revealed a good agreement between measured and simulated streamflow values with R^2 being > 0.75 for both calibration and validation periods, uncovering a decent agreement between the observed and the modeled discharge, and least error

Table 10
Weighted and ranked climate model of precipitation for each climate station.

		Wet season				Dry season					
Station ID	Adopted ID	Wcorr	Wrmse	Wsstd	STWW	Wcorr	Wrmse	Wsstd	STWD	TWWD	RANK
	CCL1	1.24	4.96	8.56	10.33	3.89	5.44	9.26	5.58	15.91	1
17025BEK	REM3	3.30	4.34	9.18	11.78	2.28	1.83	6.50	3.18	14.96	2
	RCA2	3.15	5.78	7.04	11.18	1.63	1.67	6.61	2.97	14.15	3
	RCA4	5.05	5.88	6.31	12.07	1.24	5.33	7.63	4.26	16.33	1
23018ASA	HIR	2.34	4.59	9.85	11.75	0.67	4.00	9.93	4.38	16.13	2
	CCL2	2.75	5.71	6.99	10.81	1.62	5.63	6.09	4.00	14.81	3
	RCA1	1.97	5.41	7.56	10.46	1.24	5.33	7.63	4.26	14.72	1
18026ATI	RCA4	2.83	5.46	8.37	11.67	0.75	0.96	6.22	2.38	14.05	2
	RCA5	1.17	3.92	9.78	10.41	1.20	2.74	8.11	3.61	14.02	3
	CRC2	2.20	5.56	7.56	10.72	0.27	4.52	8.73	4.05	14.77	1
23001AXM	RCA7	1.30	5.62	6.05	9.08	1.06	4.62	9.07	4.42	13.50	2
	CRC1	0.98	5.62	6.05	8.85	1.14	5.19	7.96	4.29	13.14	3
	RAC1	0.92	5.22	7.73	9.71	3.71	5.85	6.56	4.84	14.54	1
17015DUN	RCA3	1.24	4.83	8.82	10.42	0.26	5.48	6.52	3.68	14.10	2
	RCA1	0.41	5.30	7.27	9.08	1.70	5.49	7.28	4.34	13.42	3
	RAC1	1.73	5.27	8.10	10.57	3.49	5.85	6.69	4.81	15.38	1
19017EFF	RCA3	1.62	3.65	9.18	10.12	1.85	5.62	6.89	4.31	14.42	2
	RCA4	1.00	4.77	8.77	10.18	2.31	3.04	7.95	3.99	14.17	3
	REM1	1.80	5.22	8.31	10.74	2.48	4.15	9.41	4.81	15.55	1
21020KIB	REM4	2.01	5.22	8.44	10.98	2.26	3.47	8.67	4.32	15.29	2
	RCA6	0.77	5.22	7.70	9.59	2.13	5.26	8.36	4.72	14.31	3
	RCA1	0.19	4.44	8.98	9.53	3.17	5.70	7.84	5.01	14.54	1
19007KON	RCA4	2.09	4.22	9.70	11.21	1.66	0.59	5.40	2.30	13.50	2
	RCA3	2.21	2.96	7.85	9.11	1.72	5.63	6.59	4.18	13.30	3
	CCL2	0.83	4.37	9.41	10.22	0.26	5.40	6.97	3.79	14.01	1
17009KSI	RCA3	1.31	3.39	8.95	9.55	1.61	6.30	6.67	4.37	13.93	2
	RCA1	0.74	5.17	7.86	9.64	0.58	5.41	7.04	3.91	13.54	3
	CRC1	0.71	4.03	9.93	10.27	3.08	3.00	7.50	4.07	14.34	1
14044MPR	RAC2	1.33	5.62	6.22	9.22	2.40	5.33	8.38	4.83	14.05	2
	CCL3	2.20	3.05	8.05	9.31	2.04	5.50	7.48	4.51	13.81	3
	CCL1	1.46	5.27	7.93	10.26	0.90	5.35	7.38	4.09	14.35	1
21088ODA	RCA4	0.85	5.56	6.44	8.99	2.24	5.18	8.70	4.84	13.83	2
	CCL2	0.04	4.67	8.01	8.91	1.50	5.56	8.93	4.80	13.70	3
	CRC1	3.49	4.67	9.56	12.40	1.25	−0.14	4.75	1.76	14.16	1
23023TWI	RAC2	1.97	5.56	7.38	10.43	0.40	3.18	9.07	3.80	14.23	2
	RCA1	0.70	4.96	8.22	9.72	1.35	4.96	7.72	4.21	13.93	3
	RCA1	0.91	5.10	8.08	9.86	1.81	5.40	7.78	4.50	14.36	1
18015BEK	CRC1	4.38	4.74	9.09	12.74	1.30	−0.58	4.29	1.50	14.25	2
	REM1	1.37	4.18	9.93	10.83	0.92	1.26	6.53	2.61	13.44	3
	RCA1	3.46	5.82	6.49	11.04	0.13	5.44	8.30	4.16	15.20	1
23022SAL	RCA3	3.62	5.81	6.96	11.48	1.10	5.44	8.30	4.45	15.93	2
	REM4	0.43	4.36	9.23	9.82	1.01	2.59	3.02	1.99	11.80	3
	CRA1	2.42	4.00	9.16	10.90	1.20	4.68	5.22	3.33	14.23	1
22024TAF	RAC2	1.58	5.61	6.56	9.62	0.13	4.17	9.33	4.09	13.71	2
	RCA1	0.59	3.63	9.63	9.69	0.27	4.33	9.22	4.15	13.84	3
	RAC1	1.53	5.62	6.60	9.62	4.30	5.67	9.09	5.72	15.33	1
23003TDI	RCA7	1.68	5.62	5.86	9.21	1.51	0.49	5.33	2.20	11.41	2
	RCA3	2.10	5.33	8.22	10.96	0.53	0.00	0.04	0.17	11.13	3
	RCA3	3.09	3.40	7.49	9.79	0.57	5.52	6.36	3.73	13.52	1
20009FOS	RAC2	0.49	5.44	6.82	8.92	1.05	4.74	8.93	4.42	13.33	2
	REM4	1.386	2.156	7.333	7.612	0.261	2.558	9.268	3.626	11.238	3

Where Wcorr is weighted correlation, Wrmse is weighted root mean square error, Wsstd is normalized standardized deviation, STWW is scaled total weights and TWWD = STWW (wet) + STWW (dry).

variance between the two data sets (Moriasi et al., 2007). Moreover, NSE values of > 0.75 and PBIAS values inside the scope of ±10 %, demonstrates very good performance of the model. The dependability of the model was additionally affirmed by RSR values of less than 0.53 (Table 5).

In spite of the fact that the SWAT is suited for other assessment, it overestimated the measured discharge by 4.3 % and 1% during the calibration and validation respectively, with the low-magnitude values showing a good performance of the model. The overestimation is portrayed by the negative PBIAS value. The discharge hydrographs (Fig. 4) also revealed inconsistencies in the peak timings. Similar calibration concerns were faced by Abubakari et al. (2018); Aich et al. (2016), and Cornelissen et al. (2013), when they used the SWAT model in the same climatic region. This may be attributed to; limitations in the quality of observed flow data, lack of management practices in agricultural land-use and management information and exclusion of dams, reservoirs, irrigation systems and ponds during the model setup due to absence of storage capacity data. Additionally, overestimation of the streamflow may be due to

Table 11
Weighted and ranked climate model of maximum temperature for each climate station.

		Wet season				Dry season					
Station ID	Adopted ID	Wcorr	Wrmse	Wsstd	STWW	Wcorr	Wrmse	Wsstd	STWD	TWWD	RANK
	REM1	4.02	3.63	7.78	7.72	6.32	6.52	8.96	10.90	18.62	1
17025BEK	RCA8	3.50	5.63	8.37	8.75	5.33	6.24	8.00	9.78	18.54	2
	RAC2	5.46	6.08	6.74	9.14	5.44	6.15	7.10	9.34	18.48	3
	RCA1	5.11	3.63	7.04	7.89	5.24	4.67	8.99	9.45	17.34	1
23018ASA	RCA6	4.82	4.00	7.72	8.27	3.56	5.07	9.26	8.94	17.21	2
	HIR	3.71	4.41	9.04	8.58	2.57	1.85	8.96	6.69	15.27	3
	CCL2	1.37	2.07	7.22	5.34	0.96	3.14	8.48	6.29	11.63	1
18026ATI	RCA6	0.60	1.57	7.00	4.58	0.49	2.44	7.89	5.41	10.00	2
	RCA8	1.26	−0.89	3.92	2.15	3.63	5.71	6.11	7.72	9.87	3
	RCA6	3.44	5.85	6.82	8.05	4.87	5.28	9.68	9.92	17.97	1
23001AXM	CCL3	2.10	5.63	6.30	7.01	4.61	5.58	9.61	9.90	16.92	2
	HIR	4.26	5.69	5.89	7.92	4.30	6.00	7.41	8.86	16.77	3
	REM5	0.90	4.74	8.85	7.24	0.22	3.85	9.89	6.98	14.22	1
17015DUN	REM3	1.41	5.56	6.86	6.91	0.92	5.16	8.00	7.04	13.95	2
	REM2	0.62	2.69	7.37	5.34	0.40	4.30	9.33	7.01	12.36	3
	RCA6	5.32	4.30	7.63	8.62	2.59	3.89	8.96	7.72	16.34	1
19017EFF	CCL2	2.16	4.30	8.96	7.71	1.55	3.78	9.33	7.33	15.04	2
	RCA7	3.53	4.30	8.96	8.39	0.28	3.20	9.48	6.48	14.87	3
	RCA1	6.82	5.78	6.89	9.74	5.32	5.93	6.40	8.82	18.57	1
21020KIB	REM5	5.68	1.85	8.74	8.14	5.74	6.22	7.11	9.53	18.28	2
	CRC1	5.78	5.85	7.26	9.45	3.04	5.96	6.56	7.78	17.22	3
	CCL1	2.51	3.89	8.78	7.59	1.92	4.81	9.19	7.96	15.55	1
19007KON	RCA4	3.61	5.85	6.82	8.14	0.45	5.50	6.39	6.17	14.30	2
	REM4	3.06	3.18	7.68	6.96	1.23	5.26	7.89	7.19	14.15	3
	RCA1	6.06	4.44	7.67	9.09	4.13	5.67	8.89	9.34	18.43	1
17009KSI	CRC1	5.09	3.28	6.67	7.52	1.01	9.60	8.59	9.60	17.12	2
	RCA6	5.14	2.67	5.89	6.85	3.15	5.20	9.22	8.78	15.63	3
	RCA7	4.56	5.29	9.86	9.85	3.09	5.33	8.99	8.71	18.56	1
14044MPR	CRS1	4.40	4.37	8.52	8.64	4.15	5.48	9.30	9.46	18.11	2
	RCA6	5.48	4.93	8.56	9.48	3.66	5.20	6.30	7.58	17.06	3
	RCA8	5.39	5.70	9.93	10.51	5.24	6.17	8.30	9.86	20.37	1
21088ODA	RCA8	6.13	6.33	9.33	10.90	3.40	5.69	8.15	8.62	19.52	2
	RCA1	4.62	5.93	8.59	9.57	4.60	6.07	7.26	8.96	18.53	3
	RCA7	5.84	6.37	8.61	10.41	6.37	6.56	8.07	10.50	20.91	1
23023TWI	REM5	2.61	4.56	9.93	8.55	3.56	5.63	8.26	8.72	17.27	2
	REM1	3.10	3.85	8.59	7.77	3.89	5.44	9.29	9.31	17.09	3
	RAC2	2.56	5.70	7.17	7.72	3.69	5.48	8.83	9.00	16.72	1
18015BEK	RCA7	1.93	5.20	8.44	7.79	1.63	5.07	9.41	8.05	15.84	3
	RCA8	2.49	4.30	9.22	8.00	3.13	4.08	8.93	8.07	16.07	2
	CCL2	0.39	9.44	8.28	9.05	0.54	5.39	7.20	6.57	15.62	1
23022SAL	HIR	1.89	9.48	1.62	6.49	3.00	5.70	7.63	8.17	14.66	2
	RCA3	2.32	9.11	−0.33	5.55	2.94	4.70	9.93	8.78	14.33	3
	CCL3	3.80	5.33	9.44	9.29	4.21	5.63	9.04	9.44	18.73	1
22024TAF	RAC2	3.03	4.74	9.93	8.85	4.10	5.85	8.30	9.13	17.98	2
	HIR	4.75	6.07	7.89	9.36	3.27	5.73	7.76	8.38	17.74	3
	REM2	3.55	5.25	9.41	9.10	3.25	5.63	7.73	8.31	17.41	1
23003TDI	REM1	2.23	5.04	8.96	8.11	2.65	5.67	7.44	7.88	16.00	2
	RCA7	3.52	2.67	6.84	6.51	4.05	5.93	7.85	8.91	15.43	3
	RCA6	1.40	4.67	9.16	7.62	1.26	4.52	9.41	7.60	15.21	1
20009FOS	RCA1	0.20	4.37	9.11	6.84	1.86	5.11	8.39	7.68	14.52	2
	RCA4	2.37	5.63	7.63	7.81	0.68	5.43	6.96	6.53	14.35	3

Where Wcorr is weighted correlation, Wrmse is weighted root mean square error, Wsstd is normalized standardized deviation, STWW is scaled total weights and TWWD = STWW (wet) + STWW (dry).

baseflow overestimation which could result from excess aquifer contribution to groundwater recession flow in the PRB, a condition which is not dealt with in SWAT

3.3. Precipitation bias correction

The DM method moderately underestimated or overestimated the average monthly simulated RCM precipitation (Table 6) with the different scale and shape parameters (Table 7). The raw simulated data diverged from the measured precipitation in all RCM data. In addition, all the RCMs with exception of REMO, CRCM5, RACMO22 T, RCA6, RCA7and RCA8 underestimated the raw simulation mean and the 90th percentile precipitation. The DM method enhanced the raw simulation data and decreased the error in various component with various ranges.

Table 12
Weighted and ranked climate model of minimum temperature for each climate station.

		Wet season				Dry season					
Station ID	Adopted ID	Wcorr	Wrmse	Wsstd	STWW	Wcorr	Wrmse	Wsstd	STWD	TWWD	Rank
	RCA1	5.57	7.85	2.60	8.01	8.78	3.76	1.41	6.97	14.98	1
17025BEK	REM5	5.97	9.21	5.21	10.19	5.56	0.59	3.25	4.70	14.89	2
	CRC2	6.53	7.74	6.38	10.32	4.71	1.11	2.97	4.40	14.72	3
	REM1	6.69	6.67	8.97	11.16	6.03	6.60	8.44	10.53	21.69	1
23018ASA	RCA1	5.47	6.22	9.95	10.82	6.42	5.74	8.74	10.45	21.27	2
	REM5	4.63	6.05	8.08	9.38	6.15	6.67	8.22	10.52	19.90	3
	REM1	2.06	4.15	9.63	7.92	7.67	7.16	8.95	11.89	19.80	1
18026ATI	RCA1	4.31	5.93	8.22	9.23	5.11	5.72	9.70	10.27	19.50	2
	CRC1	4.14	5.94	7.70	8.89	3.94	5.89	6.78	8.30	17.19	3
	REM5	2.02	5.63	6.53	7.09	6.84	6.52	9.86	11.61	18.70	1
23001AXM	RAC1	4.60	5.73	6.00	8.16	4.91	6.27	6.96	9.07	17.24	2
	RCA3	3.25	5.70	6.30	7.62	4.99	6.15	8.06	9.60	17.22	3
	REM1	0.65	5.49	6.71	6.42	2.89	5.70	7.38	7.98	14.41	1
17015DUN	RCA3	1.43	5.25	7.89	7.29	1.65	5.63	5.88	6.58	13.87	2
	REM3	1.84	5.29	8.11	7.62	0.70	5.51	6.15	6.18	13.80	3
	RAC2	3.39	4.50	9.33	8.61	3.62	4.81	9.85	9.14	17.76	1
19017EFF	RCA6	4.02	3.47	7.56	7.53	2.12	5.35	9.00	8.23	15.76	2
	RCA4	3.28	5.35	9.00	8.81	0.22	3.78	9.26	6.63	15.44	3
	RCA7	3.05	4.75	9.98	8.89	1.69	4.26	9.99	7.97	16.86	1
21020KIB	RCA6	1.46	4.44	9.63	7.77	1.46	4.44	9.58	7.75	15.51	2
	REM4	1.53	5.05	8.58	7.58	1.53	5.03	8.60	7.58	15.16	3
	RCA5	2.05	5.47	7.78	7.65	2.74	4.89	9.56	8.59	16.24	1
19007KON	CRC2	0.99	5.42	7.29	6.85	2.84	5.50	8.17	8.25	15.10	2
	CCL3	0.90	5.33	7.45	6.84	2.28	5.07	8.89	8.12	14.96	3
	RAC1	5.39	6.22	8.37	9.99	4.36	5.30	9.95	9.81	19.80	1
17009KSI	CRC2	5.62	5.78	9.93	10.66	3.42	4.74	9.67	8.91	19.57	2
	CRC1	4.32	5.26	10.00	9.79	3.69	4.83	9.71	9.12	18.90	3
	CRC1	4.55	5.48	9.78	9.90	3.09	5.69	7.85	8.31	18.21	1
14044MPR	REM4	3.66	4.81	9.70	9.08	2.13	5.21	8.56	7.95	17.03	2
	RAC2	3.32	5.61	8.16	8.55	3.47	5.84	7.26	8.29	16.83	3
	RCA3	5.72	5.95	9.85	10.76	5.13	6.07	8.82	10.01	20.77	1
21088ODA	RAC1	6.79	6.74	8.33	10.93	5.21	6.18	7.72	9.55	20.49	2
	CRC1	5.89	5.63	9.29	10.40	4.84	6.08	8.24	9.58	19.98	3
	RCA1	4.37	5.93	8.22	9.26	5.12	5.83	9.56	10.25	19.51	1
23023TWI	CRC1	4.18	5.94	7.76	8.94	4.55	5.96	6.74	8.62	17.56	2
	RCA7	2.39	5.49	7.84	7.86	4.32	5.78	9.04	9.57	17.42	3
	RCA3	5.74	6.22	9.19	10.58	4.73	5.44	9.48	9.83	20.40	1
18015BEK	CRC1	5.82	5.89	9.93	10.82	3.65	5.33	9.26	9.12	19.94	2
	RAC1	4.96	6.11	8.33	9.70	4.07	5.41	9.48	9.48	19.18	3
	RCA3	4.18	5.78	8.62	9.29	3.72	5.52	8.94	9.09	18.38	1
23022SAL	RAC1	4.46	6.00	7.89	9.18	2.10	4.47	9.93	8.25	17.43	2
	CRC1	2.74	5.05	9.26	8.52	2.46	4.83	9.48	8.39	16.91	3
	REM5	4.34	5.48	9.50	9.66	6.24	6.15	9.99	11.19	20.85	1
22024TAF	RCA3	6.21	6.52	8.59	10.66	5.18	6.18	8.33	9.85	20.51	2
	RAC1	7.03	6.67	7.59	10.65	5.65	6.22	7.19	9.53	20.18	3
	CRC1	4.18	5.83	9.16	9.58	3.31	5.59	8.37	8.64	18.22	1
23003TDI	RAC1	3.97	5.93	7.63	8.76	4.48	5.96	8.15	9.29	18.05	2
	RCA2	4.66	5.93	8.59	9.59	2.59	4.44	9.71	8.37	17.97	3
	RCA5	5.50	6.22	7.24	9.48	4.56	6.06	8.74	9.68	19.16	1
20009FOS	RCA3	4.01	5.70	7.10	8.41	4.16	6.10	8.00	9.13	17.54	2
	CRC1	5.37	6.15	7.19	9.35	2.51	5.56	8.30	8.19	17.54	3

Where Wcorr is weighted correlation, Wrmse is weighted root mean square error, Wsstd is normalized standardized deviation, STWW is scaled total weights and TWWD = STWW (wet) + STWW (dry).

Table 13
Percentage changes in monthly and annual mean temperature under different climate models groups.

	Jan	Feb	Mar	Apr	May	Jun	Jul	Aug	Sep	Oct	Nov	Dec	Annual
Scenario	RCP4.50												
BNE4.5	6.97	3.79	1.11	3.09	0.26	1.25	0.41	2.71	4.19	4.37	3.87	5.47	2.95
BMD4.5	6.80	4.29	2.31	1.97	3.33	4.67	4.14	6.14	6.53	5.49	4.25	6.03	4.65
BED4.5	8.14	4.81	2.78	2.47	3.12	4.12	3.48	5.61	6.49	6.08	5.06	7.16	4.96
SNE4.5	4.57	6.39	3.11	6.40	4.72	9.72	9.35	10.63	9.06	8.50	5.78	6.72	7.03
SMD4.5	6.69	4.63	3.31	3.47	4.44	4.86	4.79	6.05	6.04	8.78	4.28	5.62	4.99
SED4.5	8.14	4.81	2.78	2.47	3.12	4.12	3.48	5.61	6.49	6.08	5.06	7.16	4.53
TNE4.5	6.37	3.03	1.50	1.02	2.46	1.11	1.12	4.21	5.33	5.59	4.94	6.22	3.41
TMD4.5	6.32	3.27	3.02	2.21	2.72	3.28	4.23	5.96	5.85	7.86	4.35	6.38	4.37
TED4.5	8.93	4.65	3.65	2.05	1.73	0.63	1.90	4.91	6.19	6.49	6.63	8.99	4.82
	RCP8.5												
BNE8.5	4.01	4.28	3.94	1.22	1.27	3.43	3.38	3.70	4.11	3.99	4.03	4.18	3.45
BMD8.5	8.82	6.33	5.47	5.20	5.56	7.41	5.93	7.06	6.43	6.16	5.33	7.58	6.37
BED8.5	10.03	8.44	9.50	7.66	8.31	9.82	7.65	8.22	8.54	9.06	8.21	8.38	8.66
SNE8.5	6.01	3.75	2.33	3.89	2.76	3.00	1.88	4.22	3.56	4.66	3.46	4.98	3.72
SMD8.5	9.25	6.17	5.35	5.40	6.27	7.68	7.02	6.10	6.68	5.93	5.16	6.40	6.44
SED8.5	9.00	9.41	9.26	8.69	10.45	10.48	9.72	9.15	9.26	9.05	8.07	9.94	9.33
TNE8.5	7.20	4.60	2.89	1.82	1.49	0.70	3.29	4.02	3.91	6.28	6.02	5.86	4.00
TMD8.5	8.42	7.60	5.27	9.02	5.11	8.20	5.28	6.70	6.62	6.03	5.44	7.79	6.75
TED8.5	14.19	10.35	9.49	9.85	7.28	9.64	8.94	8.08	8.98	8.96	8.51	12.56	9.74

The statistical indicators revealed uncertainty in various simulated raw RCM data. A lesser correlation coefficient (R) and a greater RMSE were revealed in entirely raw simulation. Furthermore, the DM method showed a parallel and good R in monthly mean precipitation. While reasonably similar and almost zero bias and RMSE were identified for the bias-corrected data. The outcome showed that the DM method has a good capability in adjusting the raw simulation to reproduced the observed in various aspects.

3.4. Temperature bias correction

The simulated raw temperature data overestimated the mean and 90th percentile of maximum and minimum temperature in all the RCMs apart from CCLM4−8-17 and RACM022 T (Tables 8 and 9). The R and bias of the simulated raw data were moderately good in all the RCMs simulations. Nevertheless, a moderately higher RMSE was identified in all the simulated raw maximum and minimum temperature. This result is similar to the studies by Geleta and Gobosho (2018) in Finchaa watershed, Ethiopia and Zhang et al. (2018) in northern part of Lake Erie Basin in Canada

3.5. Selection of RCMs using weighting and ranking

Fig. 5 shows samples of Taylor diagrams for only Kumasi and Takoradi, three out of the seventeen climate stations (to reduce the number of Taylor diagrams) for maximum and minimum temperature, and precipitation data. The observed data for 1970–2005 were compared with corresponding historical data obtained from individually RCMs to evaluate the CC, NRMSE, and NSD. Tables 10–12 show the weighting of the CC, NRMSE, and NSD, scaling the total weight and ranking of the first three best regional climate models for each gauge station. The results revealed that the model that reproduced the observed data best varied from one station to station. Therefore, using one RCM for climate impact assessment especially over a large area may affect the results. This may be due to the fact that each station has different land surface, vegetation dynamics, sulphate aerosol, non-sulphate aerosol, carbon concentration and atmospheric chemistry, and the models resolve these features differently. Weighting and ranking method is needed when dealing with a large area where the climate gauge stations are wide apart. The first three best RCMs for each station were used as input data for the SWAT modeling simulation in this research.

3.6. Projected climate change assessment

3.6.1. Projected temperature

Post-bias correction reveals an increment in projected temperature under RCP4.5 and RCP8.5 climate scenarios (Table 13). An increasing trend in the mean annual temperature change pattern was identified in B, S, and T across the three time periods under both scenarios. The mean yearly increase in temperature varies from + 2.9 to + 7.03 % under RCP4.5 and from + 3.5 to + 9.7 % under RCP8.5 climate scenarios. In general, the average yearly temperature increases up to 4.6 % under RCP4.5 and 6.5 °C under RCP8.5 climate scenarios over the next 90 years. According to the monthly assessment, a consistent upsurge was identified in all the months for temperatures for the two climate scenarios under the three classified time periods where January appeared to be the warmest. Furthermore, the projected increase in RCP8.5 temperature data under Africa−CORDEX climate scenarios in PRB was higher than that of the RCP4.5. The projected changes in annual and monthly temperature time scales reveal possible warmer periods in the future with RCP8.5 appeared higher. These findings are consistent with other studies carried out by Jin et al. (2018) in the Volta River Basin, Wu et al. (2017) in Jiangsu Province, Morán-Tejeda et al. (2015) in Aragón catchment and Yira et al. (2017) in Dano catchment, where

increases in temperature are expected in the NE, MD and ED.

Further assessment indicated that the RCP8.5 scenario projected higher temperatures than RCP4.5 except in the case of NE of S (SNE). The analysis depicted that with the same climate change scenario, T projected the highest temperatures for both RCP8.5 and RCP4.5.

3.6.2. *Projected precipitation*

The outcome of the post-bias corrections of precipitation data revealed general increases in future average yearly precipitation in NE and MD and decreases in the ED over PRB (Fig. 6). The increasing change in average yearly precipitation varies from + 1.2 to + 3.3 % for RCP8.5 and to a higher range of + 2.5 - + 6.5 % for RCP4.5 climate scenarios throughout the studied periods. For the reduction, RCP4.5 appeared to decrease more (-2- -4.7 %) compare to that of RCP8.5 (−1.1 to −0.84 %). The monthly precipitation assessment showed that increase in precipitation in RCP8.5 was lower than recorded in RCP4.5, and ranged between 0% and 17 %. The reduction in precipitation was higher in RCP8.5 than RCP4.5.

In general, the anticipated seasonal precipitation changes within -14 % to 18 % for RCP4.5 and -15 % to 17 % for RCP8.5. In the PRB, the future seasonal change in precipitation did not displayed any systematic reducing or increasing trend, comparing to that of temperature which exhibited an increasing trend under both climate scenarios for the projected future periods. These results are similar to researches done by Abubakari et al. (2018) in the White Volta River Basin (WVRB) in West Africa, Al-Safi and Sarukkalige

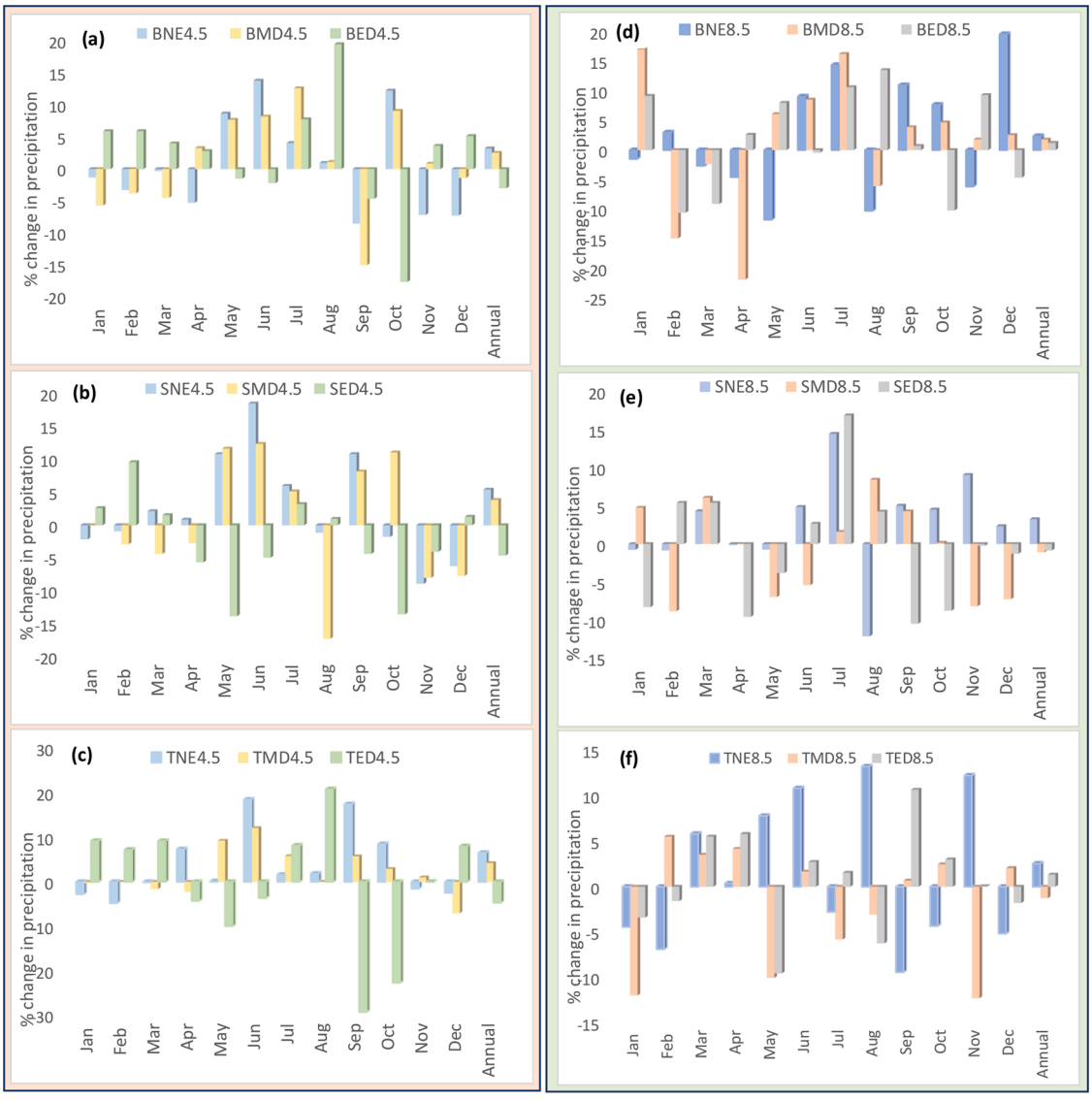

Fig. 6. Percentage changes in monthly and annual mean precipitation under different climate models groups in (a), (b), (c) RCP4.5 and (d), (e), (f) RCP8.5 emission scenarios.

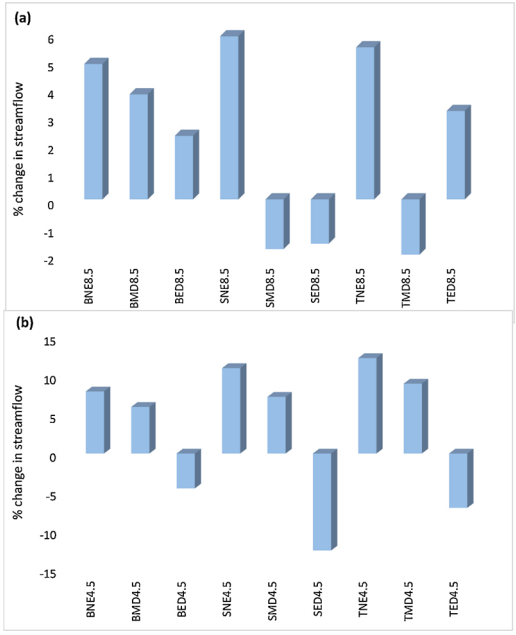

Fig. 7. Percentage change in annual streamflow in the (a) RCP8.5 and (b) RCP4.5 scenarios.

(2017) in Richmond River Catchment in New South Wales and Tall et al. (2017) in Lake of Guiers in Senegal, where climate models projected different trends of annual and monthly precipitation under different emission scenarios.

The monthly precipitation uncertainty of RCP8.5 was between 9.9 % and 11 %, 11 % and 13 %, and 12 % and 14 % in NE, MD and ED respectively. In general, the anticipated seasonal precipitation changes within -14 % to 18 % for RCP4.5 and -15 % to 17 % for RCP8.5. These results are similar to the reported results by Abubakari et al. (2018) in the WVRB in West Africa, Al-Safi and Sarukkalige (2017) in Richmond River Catchment in New South Wales and Tall et al. (2017) in Lake of Guiers in Senegal, where climate models are projecting different trends of annual and monthly precipitationl under different emission scenarios.

The uncertainties might be as a result of model construction. There are many uncertainties linked to the construction of climate models and they can be grouped into initial conditions, boundary conditions, parameterizations and model structure. Construction uncertainty is introduced by the scientific selection of model design and development.

3.7. Future streamflow changes from climate impact

The potential changes in the future streamflow under RCP4.5 and RCP8.5 for the projection periods magnitude and sign are shown in Fig. 7. All the three groups of RCMs (best, second-best and third-best) projected substantial increases in streamflow for NE and MD up to over 11 % while a reduction of about 8% was projected in ED under RCP4.5. However, RCP8.5 climate scenario revealed upsurge in streamflow that were identified for all 21 st century scenarios under B, SNE and ED of T with the highest increase of $>$ 5% projected for SNE while the highest reduction of over 2% was projected in MD of T (TMD). Increasing streamflow values were highest under the RCP4.5 emission scenario and least under RCP8.5.

The changes in the future monthly streamflow volumes under the different groups of climate models are shown in Figs. 8 and 9. In the RCP4.5 model projection, May and June depicted the same streamflow change trend; an increase in NE and MD, and a decrease in ED, while July indicated an increasing trend in all three parts of the 21 st century. The streamflow change trend in January is the same for both model groups; a decreasing trend is identified in NE and MD, and an increasing in ED. Each modeling group projected variations in the streamflow volumes. For instance, NE of B projected a 5.5 % increase in streamflow in February whereas SNE and NE of T projected reductions of 3.7 % and 8.3 % respectively for the same month. This is the same as in the month of August where B and T show increasing trends whilst S shows decreasing in all the century scenarios. Thus, the dry flow month of August may be wet under B and T modeling groups and drier under S. A shift in monthly maximum streamflow from June to July is projected by all the modeling groups for ED. Based on the results of the assessments, the projected future monthly streamflow variations as a result of the RCP4.5 will be within –15 % to 23 %.

In the case of the RCP8.5, the bias corrected B climate model group projected decreases in flow for March while S and T groups projected increments for the same month. The trend for July is similar to that of the scenario under RCP4.5 with the exception of TMD which depicted a reduction in streamflow. At peak flow in June, all the three groups of climate models showed an increase in flow up to 15 % at all the parts of the 21 st century except ED of B and MD of S which recorded reductions of 2.1 % and -9.5 % respectively. Based on the information from the RCP8.5, the projected future monthly streamflow changes may range between -24 % and 24 %.

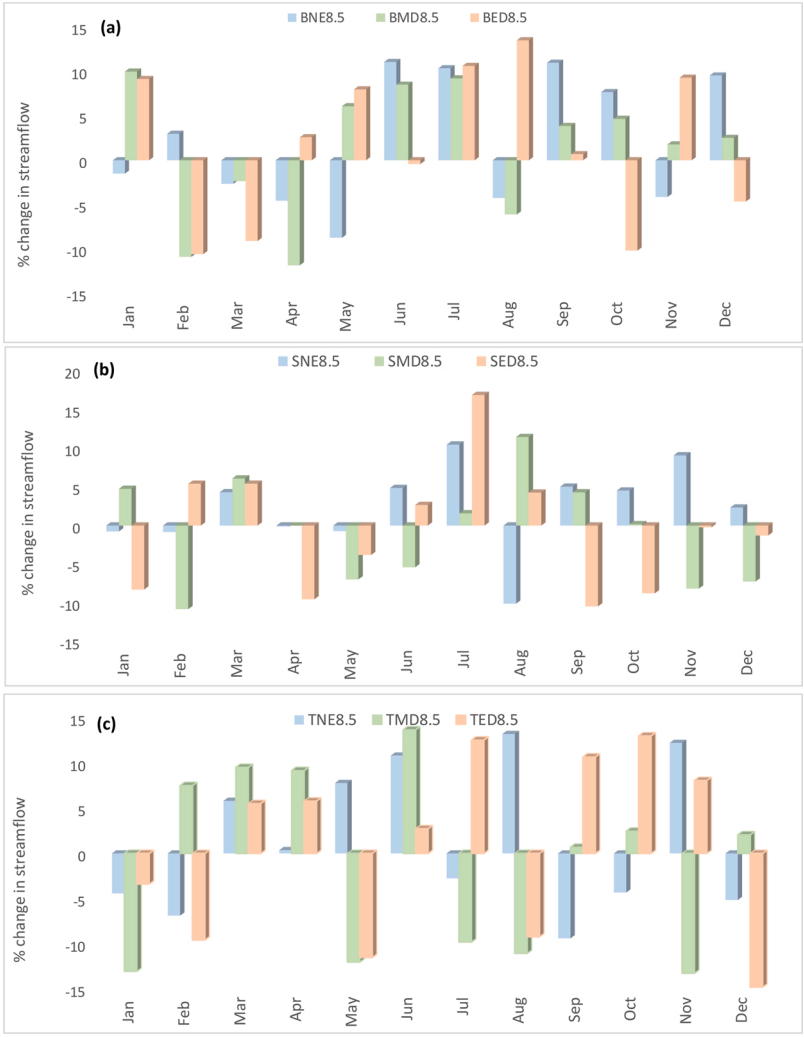

Fig. 8. Percentage change in monthly streamflow volume for RCP8.5 scenarios in the (a) near 21 st century (b) mid of 21 st century and (c) end of 21 st century.

3.8. Seasonal analysis

The overall projected streamflow changes for the wet and dry seasons show diverse patterns (Fig. 10). From the RCP8.5 results, the NEs projected streamflow changes within 2%–6% in wet season, and -6% to 10 % in the dry season. For the MDs, projected streamflow variations stretched from -4.00% to 7.00% in the wet season and from -4% to 6% in the dry season. Variations for ED ranged from -3% to 8% in the wet season and -6% to 4% in the dry season. The B modeling groups projected increasing flow volume in the wet season and decreasing flow volume in the dry season. The S modeling group depicted opposite streamflow volume change with the exception of SNE. This might be due to the different seasonal projection capabilities of the modeling groups stemming from the uncertainties in the projected future climate by the models. The magnitude and sign of the seasonal streamflow variations demonstrate noteworthy uncertainties among various modeling groups. In the RCP4.5 scenario, the patterns of the projected streamflow changes are the same in the wet season for all modeling groups; streamflow volume increased for NE and MD and decreased in ED. In general, the dry season streamflow in RCP4.5 depicted higher increasing trends compared to the trends in RCP8.5. The modeling groups B and S of RCP4.5 projected higher wet season streamflow changes than those in RCP8.5. Generally, the projected seasonal streamflow variations were not very intense for both the RCP4.5 and RCP8.5 scenarios (within -5% to 9%). The results identified in this study have also been reported by studies undertaken by Wu et al. (2017) in the Jiangsu Province, Jin et al. (2018) in the Volta River Basin, and Fentaw et al. (2018) in Ethiopian part of the Tekeze Basin.

3.9. Spatial variations of streamflow

The annual spatial distribution of the future streamflow changes across the basin revealed differences in magnitude but similarity in

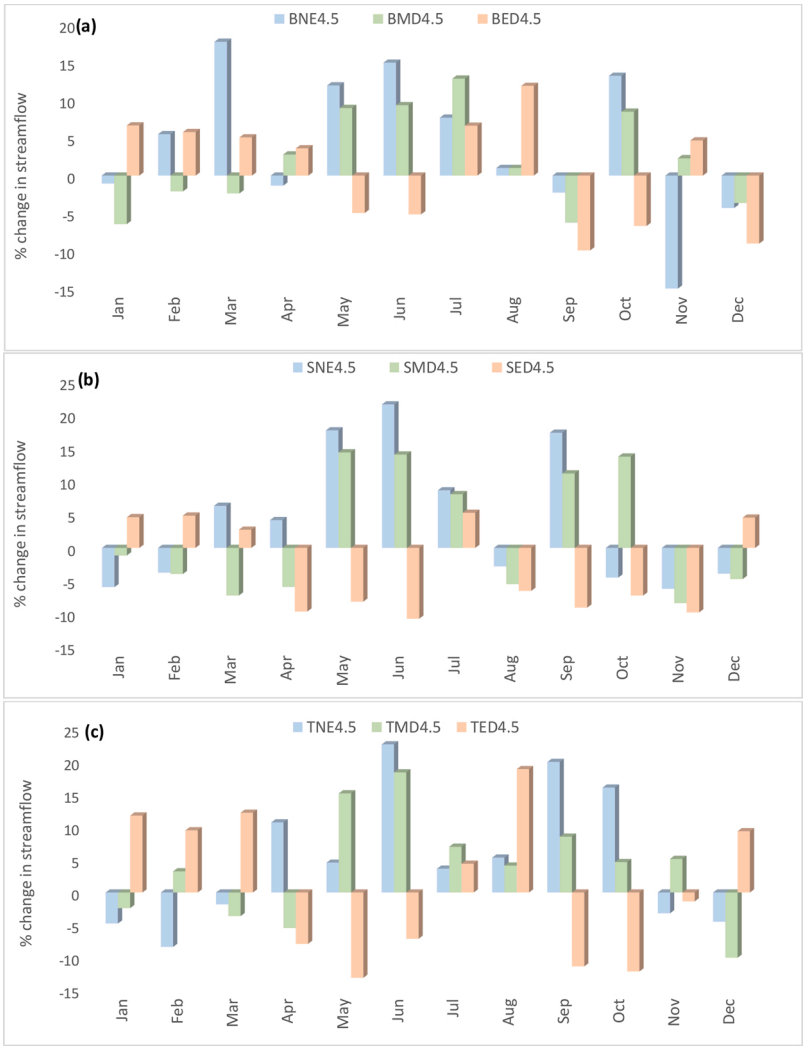

Fig. 9. Percentage change in monthly streamflow volume for RCP4.5 scenario in the (a) near 21 st century (b) mid of 21 st century and (c) end of 21 st century.

sign for the RCP4.5 scenarios (Fig. 11). The modeling groups' projections indicate reduction in streamflow in the northern sub-basins with the exception of TMD. All the modeling groups projected increases in the southern, western, eastern and middle sub-basins in the annual streamflow, apart from south-western parts of the S modeling group, and south-eastern part of TMD. In the RCP8.5 scenarios, the modeling chains projected opposite change in the northern and the upper-south sub-basins of the annual runoff when compared to the RCP4.5 (Fig. 12). The northern sub-basins revealed increase in the runoff while the upper-south indicated a decrease. Increasing runoff projections at western, eastern, middle and the southernmost sub-basins across the basin were similar to the RCP4.5 projections but different in magnitude. The moderate upsurge in mean annual streamflow for both climate scenarios, in all the future time epochs is attributed to projected increased in precipitation. Whereas the reduction in streamflow is as a result of high upsurge in projected temperature that prompts increment in evapotranspiration than upsurge in precipitation. This is in agreement with the study carried out in the WVRB where the predictions of runoff differed through modeling chains in size and trend in various parts of the basin, with the A1B emission scenario predicting increasing changes in southern and decreasing changes in northern while the B1 scenario projected the opposite (Abubakari et al., 2018). With the A1B describing a future scenario whereby there is very rapid economic growth, low population growth, and the rapid introduction of new and more efficient technologies. The variation in the energy system is not as a result of one specific energy source on the presumption that similar enhancement rates connect with all energy supply and end use technologies. Whilst B1 presumes the same population growth but with less material intensity, rapid variation in economic structures, and largely concentrates on clean and efficient technologies. It places more weight on economic, social and environmental sustainability solutions, devoid of extra climate initiatives.

The projected variations in runoff by RCPs modeling groups in the 21 st century scenarios of the basin might have dire consequences on farmers' crop yields and the operations of the Ghana Water Company Limited (GWCL), which is already faced with water availability and quality problems.

3.10. Uncertainty and limitation

These include climate models, emission scenarios, bias correction, and hydrological modelling.

Generally, the uncertainties connected to the climate model are more than those linked to the hydrological model or the bias correction (Arnell, 2011; Gosling et al., 2011; Li and Jin, 2017).

Upsurge in RCP8.5 temperature at monthly time scale through the best three models revealed uncertainty with ranges of 1.2%–3.4 %, 1.3 % to 3.76 % and 1.9 % to 4.2 % for NE, MD and ED respectively. Further assessment showed that the RCP4.5 projected higher temperatures than RCP8.5 in all the scenarios.

The uncertainties associated with the monthly precipitation at the various demarcations of the century were 8.04%–12 %, 9.1 % to 11 % and 10.6 % to 25 % in NE, MD and ED respectively. Unlike temperature variations, precipitation variations indicate much uncertainty under different RCMs and climate change scenarios.

The monthly streamflow changes from RCP8.5 (Fig. 7) indicate substantially higher uncertainties when compared RCP4.5 changes (Fig. 9). The RCP8.5 models showed monthly uncertainties varying from 7.8 % to 16 %, 9.07%–18 % and 8.5%–21 % whilst the RCP4.5 uncertainties ranged from 6.6 % to 16 %, 8.6 % to 14 % and 8.04%–14 % for NE, MD and ED respectively.

This research assumed that change in climate and anthropogenic distractions are unconnected. In reality, the alteration in climate and anthropogenic disturbances are connected and are not easily separable. So, in hydrological modeling, atmosphere-terrestrial interactions are typically very important (Li et al., 2010), which could influence the streamflow's values and distributions. Thus, further assessment of the impacts of such interactions on streamflow by means of a coupled high-resolution climate-watershed model is needed. This will be the concentration of the forthcoming research.

3.11. Climate change impact on water resources planning

The forecasted changes in PRB streamflow between 2022 and 2099 may have a remarkable effect on 43 administrative districts and it is imperative that critical reactions to these variations be considered. The projected climate variability such as the late onset of precipitation, decrease in the span of the rainy period, changes in the magnitude of precipitation and higher temperatures may affect farming schemes and GWCL operations. The PRB notably has low flood control engineering infrastructure hence future upturns in streamflow may upsurge flood challenges, and the subsequent flooding may affect water quality. It is therefore essential to plan for flood control during the raining seasons whilst drought should be mitigated during the dry season due to its impact on agricultural production. The projected higher temperatures will have an adverse impact on the water environment, and may lead to a rise in blue-green algae populations and its attendant challenges (Shang et al., 2010; Xie et al., 2016).

The GWCL stations and farmers in the basin have already adopted a wide variety of climate change adaptation techniques to continuously supply water and maintain and increase farm yields (Kankam-Yeboah et al., 2013). The existing agrarian policies or techniques must however shift towards ones which will empower farmers to better utilize the rains in the farming season. Farmers

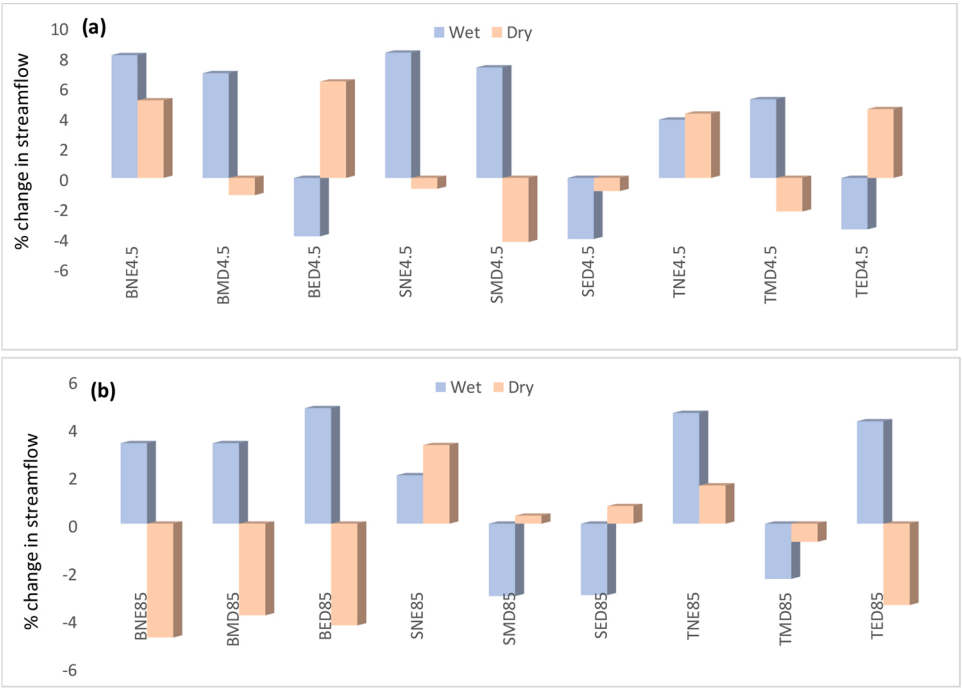

Fig. 10. Percentage change in seasonal streamflow in the (a) RCP4.5 and (b) RCP8.5 emission scenarios.

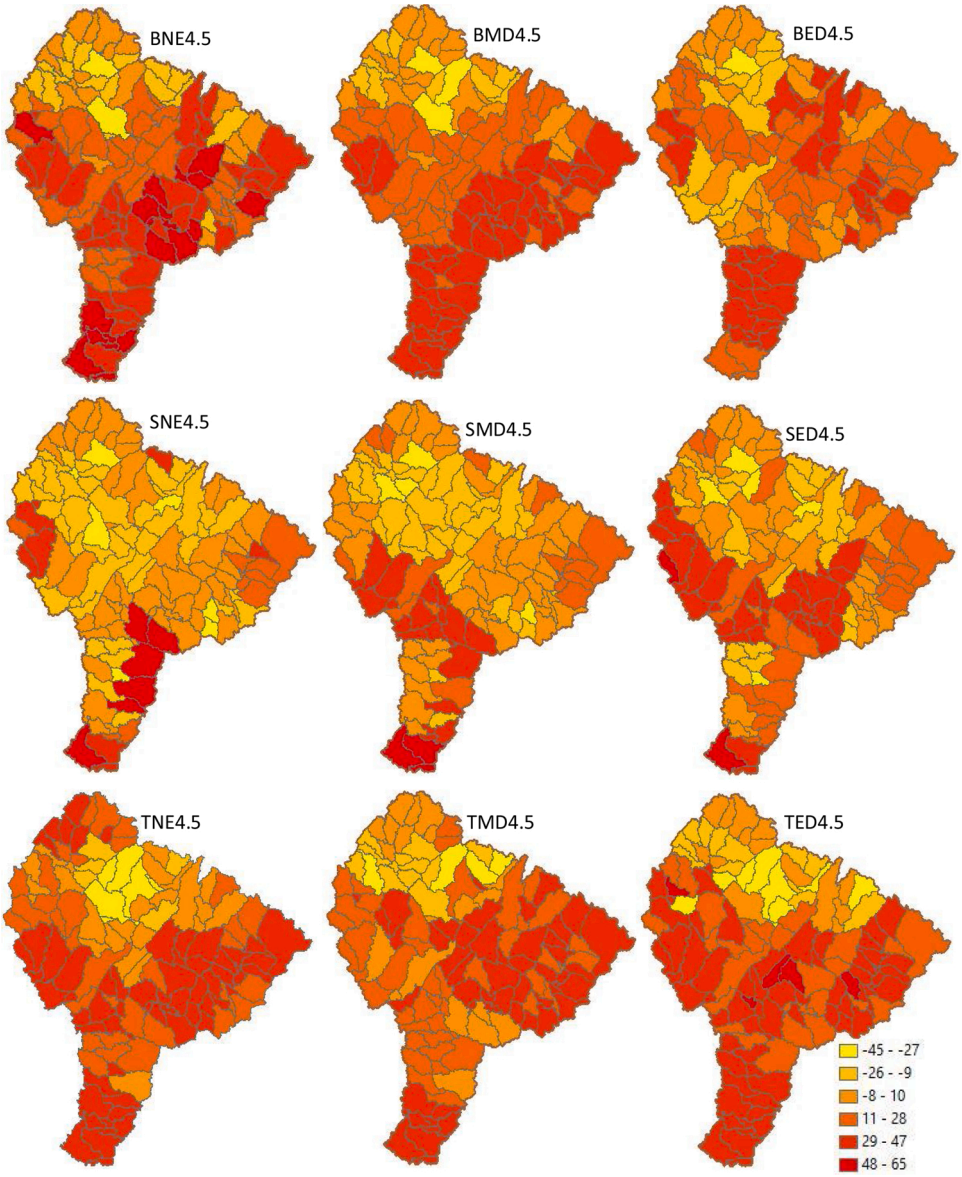

Fig. 11. Projected spatial distribution of mean annual streamflow (mm) with RCP4.5 emission scenarios.

could be advised to plant fast maturing crops, replace crops with a high-water demand with crops adjusted to the new climate variability, alter their planting period to match the new precipitation patterns, and etc. The GWCL must consider infrastructural enhancements, public education to enhance awareness of climate risks and rigorous water supply management to alleviate water stress in the basin.

From the model simulated outcomes, there are uncertainties over the sign of the change for both precipitation and streamflow in the study area. Overall, the RCP4.5 projected a decrease in runoff in the northern parts of the basin with the eastern, western, middle and southern parts expected to increase in streamflow. RCP8.5 projected an increase in streamflow in the northern, eastern, western, middle and southernmost parts of the basin, with a projected decrease in the upper-south. The proposed decrease in streamflow might have dire consequences for the operations of GWCL as well as the inhabitants of the basin whose main occupation is farming. The negative impacts of the declining water accessibility can be lessened by applying water utilization efficiency and environmental integrity as well as stepping up effective planning, management and sustenance of hydrology in these parts of the study area. Efficient utilization of water will certainly decrease demands from the three primary water use sectors: domestic supply, agriculture and industry. Keeping environmental integrity and establishing buffer zones for headwaters, wetlands, lakes and rivers would reduce the pollution and ruin of the basin's natural resources due to human factors (Awotwi et al., 2018).

The realization that mean streamflow in the PRB will increase at some part of the basin in all the modeling groups calls for suitable investments in water planning and management techniques, like construction of reservoirs that are efficient for harvesting the

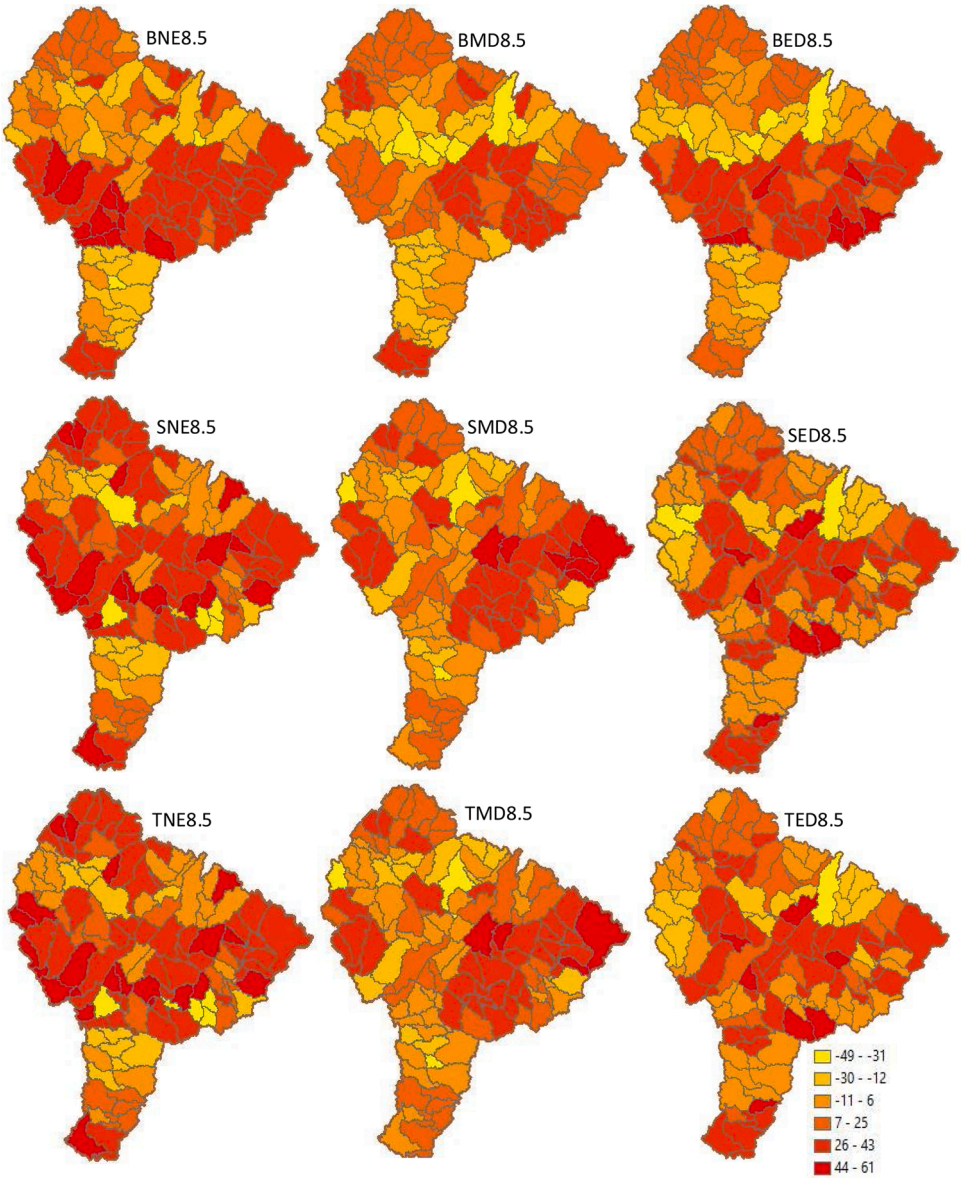

Fig. 12. Projected spatial distribution of mean annual streamflow (mm) with RCP8.5 emission scenarios.

expected increase in surface runoff. The GWCL has and will continue to increase its production due to urbanization and population growth. To achieve this aim, dams and reservoirs are being expanded or constructed. There are also small reservoirs being constructed for irrigation purposes (Water Resources Commission, 2012) with the view of storing more water in the wet season and releasing it during dry season. Regrettably, the reservoirs and dams are being designed without factoring in climate change. The designs should be enhanced by factoring in climate change impacts.

Taking the altering climate into account, it is essential to produce integrated water resource management policies that approach water storage through a variety of storage alternatives. Climate change adaptation procedures must be amalgamated with feasibility studies and development of projects for the study area (Kankam-Yeboah et al., 2013). To be sustainable, any ongoing or yet to be started project within the basin must count the possible influence of climate change on water resources and make needed provisions in planning, design and financial arrangements.

4. Conclusion

This study assessed the impacts of climate change on the PRB's streamflow using bias corrected CORDEX-Africa medium-emissions and high-emissions climate scenarios, RCP4.5 and RCP8.5, respectively. The SWAT model was deployed to simulate basin streamflow

patterns and the weighting, scaling and ranking technique was engaged to select suitable RCM combinations in order to minimize uncertainties in the climate modeling.

The MCE of the climate model for each climate station revealed that models reproducing the best of the observation dataset at each climate station are different thus, using one model output will reduce the accuracy at some stations, justifying the decision to generate and use modeling group combinations for the evaluation of the influence of climate change in the PRB

Based on the results of the modeling groups, there is consensus that the PRB is expected to experience a rise in surface runoff by the end of the 21st century. Consequently, it will be appropriate for stakeholders in agriculture in the basin and beyond to invest in cost-effective water management techniques like constructing reservoirs to harvest more water during the wet season, and gradually release it during the dry season. Agriculture policy and techniques must be geared towards those which will empower farmers to use precipitation profitably. The projected change in climate in the basin supposes that any developmental projects within the basin should factor in the possible impacts of climate change on the future water resources, and make room for planning, design and budgeting.

Though the SWAT modeling process in this study seemed quite fruitful, there are limitations in the model, being; not all the hydrological components like deep aquifer recharge or soil moisture deep aquifer recharge could be specifically calibrated due to lack of data. Also, the full capacities of the hydrological model cannot be obtained in the light of the absence of locational hydrological and farming management information.

Although outcomes of this research will offer an essential foundation for stakeholders planning for the future water resources in the PRB, there were three main uncertainties associated with the study; the static and dynamics SWAT input data, the SWAT model, and the climate model. This implies that additional research is needed to enhance the results with respect to the above uncertainties by using multiple models, and training personnel on the right way to collect, prepare and store data.

Owing to prevailing heterogeneous conditions in river basins globally, this study can be used as a guideline for other related research aimed at understanding the change and trends in water resources to advice efficient planning and management for sustaining natural resources in relation to climate change.

Authors contributions

Alfred Awotwi: Conceptualization; Methodology; Software; Validation; Investigation; Formal analysis; Resources; Data Curation; Writing - Original Draft; Writing - Review & Editing; Visualization; Funding acquisition.

Thompson Annor, Geophrey Kwame Anornu, and Jonathan Quaye-Ballard: Supervision; Validation; Investigation; Formal analysis; Writing - Review & Editing; Data Curation; Formal analysis; Resources; Data Curation

Jacob Agyekum, Boateng Ampadu, Isaac K. Nti, Maxwell Anim Gyampo and Ebenezer Boakye: Formal analysis; Project administration; Writing - Review & Editing; Data Curation.

Declaration of Competing Interest

The authors report no declarations of interest.

Acknowledgments

This study was funded by the Regional Water and Environmental Sanitation Centre, Kumasi (RWESCK) at the Kwame Nkrumah University of Science and Technology (KNUST), Kumasi, Ghana with funding from Ghana Government and the World Bank, under the Africa Centre of Excellence project

Appendix A. Supplementary data

Supplementary material related to this article can be found, in the online version, at doi:https://doi.org/10.1016/j.ejrh.2021.100805.

References

Abubakari, S., Dong, X., Su, B., Hu, X., Liu, J., Li, Y., Peng, T., Ma, H., Wang, K., Xu, S., 2018. Modeling streamflow response to climate change in data-scarce White Volta River basin of West Africa using a semi-distributed hydrologic model. J. Water Clim. Chang. jwc2018193. https://doi.org/10.2166/wcc.2018.193.

Acharya, A., Prakash, A., 2019. When the river talks to its people: Local knowledge-based flood forecasting in Gandak River basin, India. Environ. Dev. 31, 55–67. https://doi.org/10.1016/j.envdev.2018.12.003.

Aich, V., Liersch, S., Vetter, T., Fournet, S., Andersson, J.C., Calmanti, S., van Weert, F.H., Hattermann, F.F., Paton, E.N., 2016. Flood projections within the Niger River Basin under future land use and climate change. Sci. Total Environ. 562, 666–677. https://doi.org/10.1016/j.scitotenv.2016.04.021.

Akrasi, S.A., Ansa-Asare, O.D., 2008. Assessing sediment and nutrient transport in the Pra Basin of Ghana. West African. J. Appl. Ecol. 13, 1–11. https://doi.org/10.4314/wajae.v13i1.40583.

Alexandersson, H., 1986. A homogeneity test applied to precipitation data. J. Climatol. 6, 661–675. https://doi.org/10.1002/joc.3370060607.

Al-Safi, H.I.J., Sarukkalige, P.R., 2017. Assessment of future climate change impacts on hydrological behavior of Richmond River Catchment. Water Sci. Eng. 10, 197–208. https://doi.org/10.1016/j.wse.2017.05.004.

Arnell, N.W., 2011. Uncertainty in the relationship between climate forcing and hydrological response in UK catchments. Hydrol. Earth Syst. Sci. 15, 897–912. https://doi.org/10.5194/hess-15-897-2011.
Awotwi, A., Kumi, M., Jansson, P.E., Yeboah, F., Nti, I.K., 2015b. Predicting hydrological response to climate change in the White Volta catchment, West Africa. J. Earth Sci. Clim. Chang. 6, 1–7. https://doi.org/10.4172/2157-7617.1000249.
Awotwi, A., Anornu, G.K., Quaye-Ballard, J., Annor, T., Forkuo, E.K., 2017. Analysis of climate and anthropogenic impacts on runoff in the Lower Pra River Basin of Ghana. Heliyon. 3, e00477 https://doi.org/10.1016/j.heliyon.2017.e00477.
Awotwi, A., Anornu, G.K., Quaye-Ballard, J.A., Annor, T., 2018. Monitoring land use and land cover changes due to extensive gold mining, urban expansion, and agriculture in the Pra River Basin of Ghana, 1986–2025. Land Degrad. Dev. https://doi.org/10.1002/ldr.3093.
Bessah, E., Raji, A.O., Taiwo, O.J., Agodzo, S.K., Ololade, O.O., 2019. The impact of varying spatial resolution of climate models on future precipitation simulations in the Pra River Basin (Ghana). J. Water Clim. Chang. https://doi.org/10.2166/wcc.2019.258.
Cornelissen, T., Diekkrüger, B., Giertz, S., 2013. A comparison of hydrological models for assessing the impact of land use and climate change on discharge in a tropical catchment. J. Hydrol. 498, 221–236. https://doi.org/10.1016/j.jhydrol.2013.06.016.
Chu, T.W., Shirmohammadi, A., 2004. Evaluation of the SWAT model's hydrology component in the piedmont physiographic region of Maryland. Trans. ASAE 47 (4), 1057–1073. https://doi.org/10.13031/2013.16579.
Dube, K., Nhamo, G., 2019. Evidence and impact of climate change on South African national parks. Potential implications for tourism in the Kruger National Park. Environ. Dev. 100485. https://doi.org/10.1016/j.envdev.2019.100485.
Fentaw, F., Hailu, D., Nigussie, A., Melesse, A.M., 2018. Climate change impact on the hydrology of Tekeze Basin, Ethiopia: projection of rainfall-runoff for future water resources planning. Water Conserv. Sci. Eng. 3, 267–278. https://doi.org/10.1007/s41101-018-0057-3.
Geleta, C.D., Gobosho, L., 2018. Climate change induced temperature prediction and bias correction in Finchaa watershed. American-Eurasian J. Agric. Environ. Sci. 18 (6), 324–337. https://doi.org/10.5829/idosi.aejaes.2018.324.337.
Gosling, S.N., Taylor, R.G., Arnell, N.W., Todd, M.C., 2011. A comparative analysis of projected impacts of climate change on river runoff from global and catchment-scale hydrological models. Hydrol. Earth Syst. Sci. 15, 279–294. https://doi.org/10.5194/hess-15-279-2011.
Gupta, H.V., Sorooshian, S., Yapo, P.O., 1999. Status of automatic calibration for hydrologic models: comparison with multilevel expert calibration. J. Hydrol. Eng. 4 (2), 135–143. https://doi.org/10.1061/(ASCE)1084-0699(1999)4:2(135).
Hassanzadeh, E., Elshorbagy, A., Wheater, H., Gober, P., 2016. A risk-based framework for water resource management under changing water availability, policy options, and irrigation expansion. Adv. Water Resour. 94, 291–306. https://doi.org/10.1016/j.advwatres.2016.05.018.
He, J., Glotfelty, T., Yahya, K., Alapaty, K., Yu, S., 2017. Does temperature nudging overwhelm aerosol radiative effects in regional integrated climate models? Atmos. Environ. 154, 42–52. https://doi.org/10.1016/j.atmosenv.2017.01.040.
Hirpa, F.A., Dyer, E., Hope, R., Olago, D.O., Dadson, S.J., 2018. Finding sustainable water futures in data-sparse regions under climate change: Insights from the Turkwel River basin, Kenya. J. Hydrol. Reg. Stud. 19, 124–135. https://doi.org/10.1016/j.ejrh.2018.08.005.
Hu, Y., Gao, M., 2019. Evaluations of water yield and soil erosion in the Shaanxi-Gansu Loess Plateau under different land use and climate change scenarios. Environ. Dev. 100488. https://doi.org/10.1016/j.envdev.2019.100488.
IPCC, 2014. Climate change 2014. Impacts, adaptation, and vulnerability. In: Barros, V.R., Field, C.B., Dokken, D.J., Mastrandrea, M.D., Mach, K.J., Bilir, T.E., Chatterjee, M., Ebi, K.L., Estrada, Y.O., Genova, R.C., Girma, B., Kissel, E.S., Levy, A.N., MacCracken, S., Mastrandrea, P.R., White, L.L. (Eds.), Part B: Regional Aspects. Contribution of Working Group II to the Fifth Assessment Report of the Intergovernmental Panel on Climate Change. Cambridge University Press, Cambridge, UK and New York, NY, USA, pp. 1133–1820, 2014.
Jin, L., Whitehead, P.G., Addo, K.A., Amisigo, B., Macadam, I., Janes, T., Crossman, J., Nicholls, R.J., McCartney, M., Rodda, H.J., 2018. Modeling future flows of the Volta River system: impacts of climate change and socio-economic changes. Sci. Total Environ. 637, 1069–1080. https://doi.org/10.1016/j.scitotenv.2018.04.350.
Kabuya, P.M., Hughes, D.A., Tshimanga, R.M., Trigg, M.A., Bates, P., 2020. Establishing uncertainty ranges of hydrologic indices across climate and physiographic regions of the Congo River Basin. J. Hydrol. Reg. Stud. 30, 100710 https://doi.org/10.1016/j.ejrh.2020.100710.
Kankam-Yeboah, K., Obuobie, E., Amisigo, B., Opoku-Ankomah, Y., 2013. Impact of climate change on streamflow in selected river basins in Ghana. Hydrolog. Sci. J. 58, 773–788. https://doi.org/10.1080/02626667.2013.782101.
Khandekar, N., Gorti, G., Bhadwal, S., Rijhwani, V., 2019. Perceptions of climate shocks and gender vulnerabilities in the Upper Ganga Basin. Environ. Dev. https://doi.org/10.1016/j.envdev.2019.02.001.
Kumar, N., Tischbein, B., Kusche, J., Laux, P., Beg, M.K., Bogardi, J.J., 2017. Impact of climate change on water resources of upper Kharun catchment in Chhattisgarh, India. J. Hydrol. Reg. Stud. 189–207. https://doi.org/10.1016/j.ejrh.2017.07.008.
Kusimi, J.M., Amisigo, B.A., Banoeng-Yakubo, B.K., 2014. Sediment yield of a forest river basin in Ghana. Catena 123, 225–235. https://doi.org/10.1016/j.catena.2014.08.001.
Li, Z., Jin, J., 2017. Evaluating climate change impacts on streamflow variability based on a multisite multivariate GCM downscaling method in the Jing River of China. Hydrol. Earth Syst. Sci. 21 (11), 5531–5546. https://doi.org/10.5194/hess-21-5531-2017.
Mahé, G., 2009. Surface/groundwater interactions in the Bani and Nakambe rivers, tributaries of the Niger and Volta basins. West Africa. Hydrolog. Sci. J. 54, 704–712. https://doi.org/10.1623/hysj.54.4.704.
Mbaye, M.L., Haensler, A., Hagemann, S., Gaye, A.T., Moseley, C., Afouda, A., 2016. Impact of statistical bias correction on the projected climate change signals of the regional climate model Remo over the Senegal river basin. Int. J. Climatol. 36, 2035–2049. https://doi.org/10.1002/joc.4478.
Morán-Tejeda, E., Zabalza, J., Rahman, K., Gago-Silva, A., López-Moreno, J.I., Vicente-Serrano, S., Lehmann, A., Tague, C.L., Beniston, M., 2015. Hydrological impacts of climate and land-use changes in a mountain watershed: uncertainty estimation based on model comparison. Ecohydrology 8, 1396–1416. https://doi.org/10.1002/eco.1590.
Moriasi, D.N., Arnold, J.G., Van Liew, M.W., Bingner, R.L., Harmel, R.D., Veith, T.L., 2007. Model evaluation guidelines for systematic quantification of accuracy in watershed simulations. Trans. ASABE 50, 885–900. https://doi.org/10.13031/2013.23153.
Nash, J.E., Sutcliffe, J.V., 1970. River flow forecasting through conceptual models: part 1. A discussion of principles. J. Hydrol. 10 (3), 282–290. https://doi.org/10.1016/0022-1694(70)90255-6.
Noi, L.V.T., Nitivattananon, V., 2015. Assessment of vulnerabilities to climate change for urban water and wastewater infrastructure management: Case study in Dong Nai river basin, Vietnam. Environ. Dev. 16119–16137. https://doi.org/10.1016/j.envdev.2015.06.014.
Olsson, T., Jakkila, J., Veijalainen, N., Backman, L., Kaurola, J., Vehvilainen, B., 2015. Impacts of climate change on temperature, precipitation and hydrology in Finland—studies using bias corrected regional climate model data. Hydrol. Earth Syst. Sci. 19, 3217–3238. https://doi.org/10.5194/hess-19-3217-2015.
Piani, C., Weedon, G.P., Best, M., Gomes, S.M., Viterbo, P., Hagemann, S., Haerter, J.O., 2010. Statistical bias correction of global simulated daily precipitation and temperature for the application of hydrological models. J. Hydrol. 395, 199–215. https://doi.org/10.1016/j.jhydrol.2010.10.024.
Rashid, M.A., Jabloun, M., Andersen, M.N., Zhang, X., Olesen, J.E., 2019. Climate change is expected to increase yield and water use efficiency of wheat in the North China Plain. Agric. Water Manage. 222, 193–203. https://doi.org/10.1016/j.agwat.2019.06.004.
Rathjens, H., Bieger, B., Srinivasan, S., Chaubey, I., Arnold, J.G., 2016. CMhyd User Manual. Documentation for Preparing Simulated Climate Change Data for Hydrologic Impact Studies. Retrieved from http://swat.tamu.edu/software/cmhyd/ (Accessed on 26 November 2018).
Salack, S., Sarr, B., Sangare, S.K., Ly, M., Sanda, I.S., Kunstmann, H., 2015. Crop-climate ensemble scenarios to improve risk assessment and resilience in the semi-arid regions of West Africa. Clim. Res. 65, 107–121. https://doi.org/10.3354/cr01282.
Santhi, C., Arnold, J.G., Williams, J.R., Dugas, W.A., Srinivasan, R., Hauck, L.M., 2011. Validation of the swat model on a large RWER basin with point and nonpoint sources 1. JAWRA J. Am. Water Resour. Assoc. 37 (5), 1169–1188. https://doi.org/10.1111/j.1752-1688.2001.tb03630.x.
Sassi, M., Nicotina, L., Pall, P., Stone, D., Hilberts, A., Wehner, M., Jewson, S., 2019. Impact of climate change on European winter and summer flood losses. Adv. Water Resour. 129, 165–177. https://doi.org/10.1016/j.advwatres.2019.05.014.

Schilling, J., Freier, K.P., Hertig, E., Scheffran, J., 2012. Climate change, vulnerability and adaptation in North Africa with focus on Morocco. Agric. Ecosyst. Environ. 156, 12–26. https://doi.org/10.1016/j.agee.2012.04.021.

Schmidli, J., Frei, C., Vidale, P.L., 2006. Downscaling from GCM precipitation: a benchmark for dynamical and statistical downscaling methods. Int. J. Climatol. 2006 (26), 679–689. https://doi.org/10.1002/joc.1287.

Serdeczny, O., Adams, S., Baarsch, F., Coumou, D., Robinson, A., Hare, W., Schaeffer, M., Perrette, M., Reinhardt, J., 2017. Climate change impacts in Sub-Saharan Africa: from physical changes to their social repercussions. Reg. Environ. Chang. 17 (6), 1585–1600.

Shang, Z.T., Ren, J., Qin, M.R., Xia, Y., He, L., Chen, Y.W., 2010. The relationship between climatic change and blue algae eruption in Taihu Lake. China. J. Ecol. 1, 55–61. https://doi.org/10.13292/j.1000-4890.2010.0047.

Shrestha, M., Acharya, S.C., Shrestha, P.K., 2017. Bias correction of climate models for hydrological modelling–are simple methods still useful? Meteorol. Appl. 24 (3), 531–539. https://doi.org/10.1002/met.1655.

Szabó-Takács, B., Farda, A., Skalák, P., Meitner, J., 2019. Influence of Bias correction methods on simulated Köppen− Geiger climate zones in Europe. Climate 7 (2), 18. https://doi.org/10.3390/cli7020018.

Tall, M., Sylla, M.B., Diallo, I., Pal, J.S., Faye, A., Mbaye, M.L., Gaye, A.T., 2017. Projected impact of climate change in the hydroclimatology of Senegal with a focus over the Lake of Guiers for the twenty-first century. Theor. Appl. Climatol. 129, 655–665. https://doi.org/10.1007/s00704-016-1805-y.

Teutschbein, C., Seibert, J., 2012. Bias corretion of regional climate model simulations for hydrological climate change impact studies: review and evaluation of different methods. J. Hydrol. 2012, 456–457. https://doi.org/10.1016/j.jhydrol.2012.05.052.

Tschoke, G.V., Kruk, N.S., Queiroz, P.I.B., Chou, S., de Sousa, W.C., 2017. Comparison of two bias correction methods for precipitation simulated with a regional climate model. Theor. Appl. Climatol. 127, 841–852. https://doi.org/10.1007/s00704-015-1671-z.

Van Vuuren, D.P., Edmonds, J., Kainuma, M., Riahi, K., Thomson, A., Hibbard, K., Hurtt, G.C., Kram, T., Krey, V., Lamarque, J.F., Masui, T., 2011. The representative concentration pathways: an overview. Clim. Chang. 109, 5. https://doi.org/10.1007/s10584-011-0148-z.

Walker, W.E., Harremoës, P., Rotmans, J., Van Der Sluijs, J.P., Van Asselt, M.B., Janssen, P., Krayer von Krauss, M.P., 2003. Defining uncertainty: a conceptual basis for uncertainty management in model-based decision support. Integr. Assess. 4 (1), 5–17. https://doi.org/10.1076/iaij.4.1.5.16466.

Water Resources Commission, 2012. Pra River Basin - Integrated Water Resources Management Plan. Published by Ghana Water Resources Commission (GWRC). Retrieved from http://www.wrc-gh.org/dmsdocument/15. (Accessed 20/02/2017).

Wijngaard, J.B., Tank, A.K., Können, G.P., 2003. Homogeneity of 20th century Europeandaily temperature and precipitation series. Int. J. Climatol. 23 (6), 679–692. https://doi.org/10.1002/joc.906.

Wu, Z., Chen, X., Lu, G., Xiao, H., He, H., Zhang, J., 2017. Regional response of runoff in CMIP5 multi-model climate projections of Jiangsu Province, China. Stoch. Environ. Res. Risk Assess. 31, 2627–2643. https://doi.org/10.1007/s00477-016-1349-9.

Xie, X.P., Li, Y.C., Hang, X., Huang, S., 2016. The effect of air temperature on the process of cyanobacteria recruitment and dormancy in Lake Taihu. J. Lake Sci. 28, 818–824. https://doi.org/10.18307/2016.0415.

Yira, Y., Diekkrüger, B., Steup, G., Bossa, A.Y., 2017. Impact of climate change on hydrological conditions in a tropical West African catchment using an ensemble of climate simulations. Hydrol. Earth Syst. Sci. 21, 2143. https://doi.org/10.5194/hess-21-2143-2017.

Yomo, M., Mourad, K.A., Gnazou, M.D., 2019. Examining water security in the challenging environment in Togo, West Africa. Water 11 (2), 231. https://doi.org/10.3.

Zhang, B., Shrestha, N., Daggupati, P., Rudra, R., Shukla, R., Kaur, B., Hou, J., 2018. Quantifying the impacts of climate change on Streamflow dynamics of two Major Rivers of the northern Lake Erie Basin in Canada. Sustainability 10 (8), 2897. https://doi.org/10.3390/su10082897.